

MMP9 IN CYTOSKELETAL REMODELLING DURING TGF- β INDUCED
EMT

AN INVESTIGATION INTO THE ROLE OF MMP9 IN REGULATING
CYTOSKELETAL REMODELLING DURING TGF- β INDUCED EMT IN THE
LENS

By

ZI ZHEN (GINNY) LIU, BSc. (Hons.)

A Thesis

A Thesis Submitted to the School of Graduate Studies

In Partial Fulfillment of the Requirements

For the Degree

Master of Science

McMaster University

© Copyright by Zi Zhen (Ginny) Liu, August 2021

Descriptive Note

MASTER OF SCIENCE (2021)

McMaster University

(Medical Sciences)

Hamilton, Ontario

TITLE: An investigation into the role of MMP9 in cytoskeletal remodelling during TGF- β -induced EMT in the lens.

AUTHOR: Zi Zhen (Ginny) Liu, BSc. (Hons.) (Queen's University)

SUPERVISOR: Dr. Judith West-Mays

NUMBER OF PAGES: xi, x68

ABSTRACT

Fibrotic cataracts are attributed to transforming growth factor-beta (TGF- β)-induced epithelial-to-mesenchymal transition (EMT) (Eldred *et al.*, 2011). Using *in vivo* and *ex vivo* mouse knockout (KO) models, our laboratory has identified matrix metalloproteinase-9 (MMP9) as an essential protein in the EMT process. However, alternations to the cytoskeleton were observed in MMP9KO mouse lens epithelial cells (LECs) (Korol *et al.*, 2014). In addition, alpha-smooth muscle actin and filamentous actin stress fibres were absent in TGF- β 2 treated MMP9KO mouse LECs, and a NanoString analysis revealed no marked differences in *ACTA2* and *ACTB* expression between the lenses of TGF- β -overexpressing mice (TGF- β^{tg}) and TGF- β^{tg} mice on a MMP9KO background. Our laboratory subsequently conducted a cytoskeletal protein array, which revealed the differential regulation of numerous proteins in MMP9KO mouse LECs.

The purpose of this thesis is to validate select proteins from the protein array, and reveal pathways that are regulated by MMP9 during TGF- β 2-induced EMT. In order to improve the efficiency of experiments, the novel MMP9-specific inhibitor, JNJ0966, was confirmed to be able to prevent TGF- β 2-induced EMT in rat LEC explants. Cortactin, focal adhesion kinase (FAK), lim-domain kinase 1 (LIMK1) and myosin light chain 2 were selected from the array and analyzed via western blot and immunofluorescence analyses. Results from the protein array and validation studies agree for all selected proteins except for FAK. Although FAK was upregulated in rat LECs that were co-treated with JNJ0966 and TGF- β 2 (TG:JNJ), it was not activated to exert its effects. Interestingly, LIMK1 was also observed to be localized to the nucleus in JNJ0966-treated LECs. The localization of MRTF-A was also analyzed via immunohistochemistry, and we observed reduced MRTF-A nuclear translocation in TG:JNJ LECs. Results from this thesis revealed that MMP9 deficiency differentially regulated proteins

involved in actin polymerization and cell migration, and these alterations conferred resistance against TGF- β 2-induced EMT.

ACKNOWLEDGEMENTS

First and foremost, I would like to thank my supervisor, Dr. Judith West-Mays for providing me with the opportunity to learn so much about ocular diseases, a field that I have been interested in for a long time. Your careful guidance, support, patience and efficient communication skills have been instrumental to my success in the Medical Sciences program. Your knowledge, passion and impressive work ethic made and will make you a great role model and supervisor for me and future students.

A sincere thank you to Dr. Peter Margetts and Dr. Heather Sheardown for your guidance, advice and encouragement during committee meetings and throughout my degree.

I would also like to thank Dr. Aftab Taiyab for tirelessly training me to obtain rat lens epithelial cell explants and conduct other experiments needed for the completion of this thesis. I would also like to thank Paula, our lab technician, for always helping me with the endless cages of rats. I would not have been able to complete this thesis without both of your help!

Next, I would like to thank my labmates, Monica Akula, Hadyn Walker and Japnit Dham, for our interesting conversations about a seemingly endless number of random topics!

Lastly, but not least, I would like to thank my housemates in Hamilton, my close friends and my parents for always being there to listen and support me!

TABLE OF CONTENTS

Descriptive Note	ii
ABSTRACT	iii
ACKNOWLEDGEMENTS	v
LIST OF FIGURES	viii
LIST OF ABBREVIATIONS	x
CHAPTER ONE	1
General Introduction	1
1.1 Lens Anatomy	2
1.2 Fibrotic Cataracts	4
1.3 Fibrosis and the Lens as a Model for Fibrosis	6
1.4 TGF-β and Epithelial-to-Mesenchymal Transition	8
1.5 Matrix Metalloproteinases and Cytoskeletal Modifications	15
1.6 Actin Polymerization and Cytoskeletal Remodelling During TGF-β-induced EMT	16
1.7 The actin polymerization machinery may be inactive due to the lack of MMP9	20
CHAPTER TWO	25
Main Hypothesis and Specific Aims	25
2.1 Main Hypothesis	26
2.2 Specific Aims	26
2.2.1 Aim 1	26
2.2.2 Aim 2	27
2.2.3 Aim 3	27
CHAPTER THREE	28
Materials and Methods	28
3.1 Obtaining and Culturing <i>ex vivo</i> rat LEC explants	29
3.2 Treatments of rat LEC explants with TGF-β2 and JNJ0966	29
3.3 Immunofluorescence Staining	30
3.4 Western Blot Analysis	31

CHAPTER FOUR	32
Results	32
4.1 Aim 1	33
4.2 Aim 2	36
4.3 Aim 3	45
CHAPTER FIVE	47
Discussion	47
5.1 Discussion	48
5.2 Future Directions	56
5.2.1 Additional investigations of the differentially regulated proteins from the cytoskeletal protein array	56
5.2.2. Investigation into other potential MMP9-dependent pathways	56
5.2.3. Investigation into mechanisms which MMP9 regulates proteins involved in actin polymerization and cell migration	57
5.3 Conclusion	58
APPENDIX	59
A1: Treatment of Mouse LEC explants	60
A2: Phalloidin staining	60
A3: NanoString Analysis	60
A4: Cytoskeletal protein array	61
REFERENCES	62

LIST OF FIGURES

Figure 1. The anatomy of the lens.	2
Figure 2. Lens development.	3
Figure 3. Anterior subcapsular cataract (ASC).	5
Figure 4. Posterior capsular opacification (PCO).	6
Figure 5. Lens epithelial cell explant protocol.	7
Figure 6. TGF-β activation.	10
Figure 7. Epithelial-to-mesenchymal transition (EMT).	11
Figure 8. Attachment of LECs to the lens capsule.	12
Figure 9. Major TGF-β induced signalling pathways involved in EMT.	14
Figure 10. Simplified summary of potential actin polymerization pathways during TGF-β2 induced EMT.	17
Figure 11. Phalloidin staining for F-actin.	20
Figure 12. Expression of <i>MMP9</i> (A), <i>ACTA2</i> (B), and <i>ACTB</i> (C) during NanoString analysis.	22
Figure 13. Notable fold changes from the cytoskeletal protein array.	24
Figure 14. Images of LECs upon JNJ0966 treatment.	34
Figure 15. Expression and localization of E-cadherin and αSMA.	35
Figure 16. Protein expression levels of selected proteins.	38
Figure 17. Expression and localization of cortactin.	39
Figure 18. Expression and localization of focal adhesion kinase (FAK).	40
Figure 19. Expression and localization of phosphorylated focal adhesion kinase at Tyr397 (pFAK).	41

Figure 20. Expression and localization of lim-domain kinase-1 (LIMK1).	42
Figure 21. Expression and localization of phosphorylated lim-domain kinase-1 at Thr508 (pLIMK1).	43
Figure 22. Localization of phosphorylated myosin light chain-2 at Ser18 (pMLC2).	44
Figure 23. Expression and localization of myocardin-related transcription factor-A (MRTF-A).	46

LIST OF ABBREVIATIONS

α SMA	alpha smooth muscle actin
ADP	adenosine diphosphate
ASC	anterior subcapsular cataract
ATP	adenosine triphosphate
Arp2/3	actin related protein 2/3
β -catenin	beta catenin
CAM	cell adhesion molecule
Co-Smad	common partner Smad
DAPI	4',6-diamidino-2-phenylindole
DMSO	dimethyl sulfoxide
EMT	epithelial-to-mesenchymal transition
E-cadherin	epithelial cadherin
ECM	extracellular matrix
F-actin	filamentous actin
FAK	focal adhesion kinase
FITC	fluorescein-isothiocyanate
G-actin	globular actin
GAP	GTPase-activating proteins
GEF	GTP exchange factors
GSK-3 β	glycogen synthase kinase 3 beta
GTP	guanine triphosphate
ILK	integrin-linked kinase

I-Smad	inhibitory Smad
LAP	latency associated protein
LEC	lens epithelial cell
LIMK1	lim domain kinase 1
MMP	matrix metalloproteinase
MLC	myosin light chain
MLCK	myosin light chain kinase
MRTF-A	myocardin-related-transcription-factor A
PBS	phosphate buffered saline
PCO	posterior capsule opacification
PFA	paraformaldehyde
Pi	inorganic phosphate
ROCK	rho-associated coiled-coil forming protein kinase
R-Smad	receptor regulated Smad
Ser	serine
TGF- β	transforming growth factor beta
TGF- β R	transforming growth factor beta receptor
Thr	threonine
Tyr	tyrosine

CHAPTER ONE
General Introduction

1.1 Lens Anatomy

The eye is a complex structure that is derived from the embryonic mesoderm and ectoderm (Ort and Howard, n.d.). The ectoderm is specialized into the innervated neuroectoderm and the non-innervated surface ectoderm (Ort and Howard, n.d.). The lens and parts of the cornea are derived from the surface ectoderm, and the two structures are responsible for light refraction and transmission (Ort and Howard, n.d.). The lens borders the posterior and anterior segments of the eye and receives all of its nutrition from the aqueous humour in the anterior segment and the vitreous humour in the posterior segment (Eldred *et al.*, 2011).

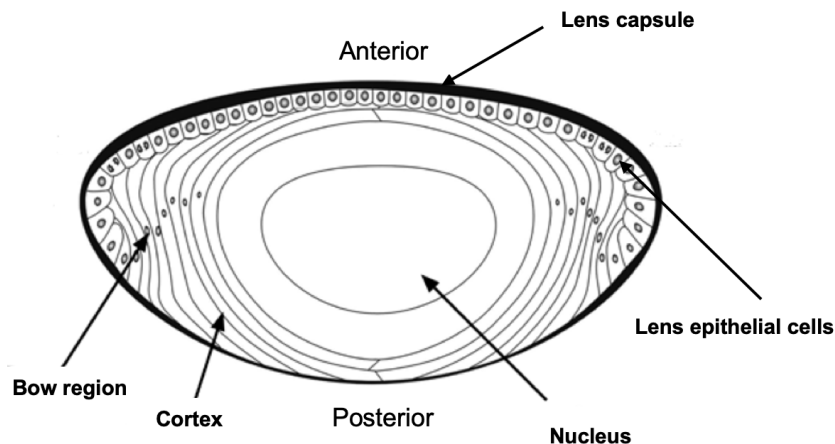


Figure 1. The anatomy of the lens. The ocular lens is a biconvex structure that is protected by its basement membrane, the lens capsule. There is a monolayer of lens epithelial cells that reside beneath the anterior capsule. These cells have the potential to divide and differentiate into lens fibre cells. The bow region consists of differentiating cells that are being added to the fibre mass, which is made up of the cortex and nucleus. Figure adapted from Raj *et al.*, 2007.

The lens is a biconvex and avascular structure (Raj *et al.*, 2007), and it has three major components: the nucleus, the cortex and the capsule (Figure 1) (Tholozan and Quinlan, 2007). There are only two types of cells in the lens, the lens fibre cells, which make up the cortex and nucleus, and the monolayer of lens epithelial cells (LECs) (Tholozan and Quinlan, 2007). Lens fibre cells, collectively known as the fibre mass, are inactive cells filled with soluble crystallin proteins that provide clarity and help transmit light (Andley, 2008). The lens capsule, which

consists of mostly collagen IV and laminin, allows the lens to keep its structural integrity and keeps the lens relatively isolated from other ocular structures (Eldred *et al.*, 2011). The lens capsule is thickened on the anterior side to protect the monolayer of LECs that reside beneath it (Eldred *et al.*, 2011). The LECs, which are the progenitors of lens fibre cells, divide and are displaced from the anterior to the equator of the lens to add to the fibre mass throughout a person's lifetime (Tholozan and Quinlan, 2007). As such, this monolayer is divided into four zones: the central zone, the pre-germinative zone, the germinative zone, and the transitional zone (Figure 2) (Šikić *et al.* 2017). The LECs receive differentiation signals, and progressively lose organelles as they are displaced from the border of the bow region to the interior cortex of the lens (Šikić *et al.*, 2017). Overall, the only cells in the ocular lens that are capable of mitosis are the LECs, and these cells are of primary interest in this thesis.

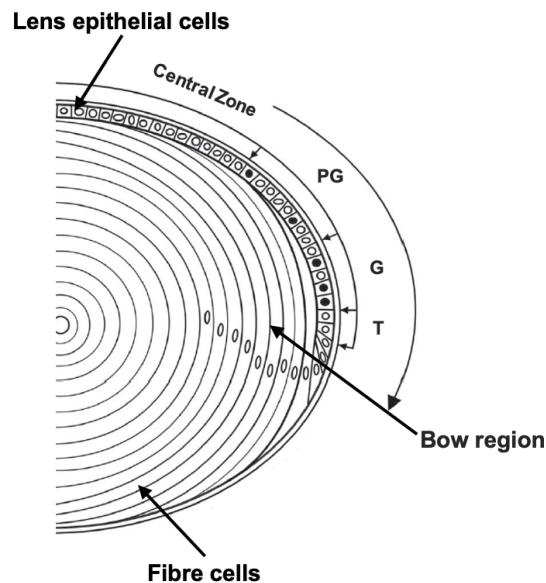


Figure 2. Lens development. Cells with black nuclei indicate cells in the S-phase. The central zone is the region of the lens epithelial cell (LEC) monolayer with non-dividing LECs arrested in the G₀ phase. The pre-germinative zone (PG) consists of LECs that have the potential to divide, and it is the site of occasional mitotic division. The germinative zone (G) is the major site of cell division. The transition zone (T) consists of cells that have completed the cell cycle but have not undergone differentiation. Cells from the T zone will continue to move to the equator of the lens and be added to the bow region, where the cells will eventually lose all their organelles and differentiate into lens fibre cells. Figure adapted from Šikić *et al.*, 2017.

1.2 Fibrotic Cataracts

Cataract is the leading cause of blindness affecting 94 million people around the world (“Vision impairment and blindness”, 2021). While there are many different types of cataracts, the treatment is often the same: cataract surgery, which involves the removal of the cataractous lens and replacement with a synthetic intraocular lens (Raj *et al.*, 2007). Although the procedure is generally deemed safe, secondary cataract can form in as low as less than 5% and as high as 50% of the patients (Raj *et al.*, 2007). Anterior subcapsular cataract (ASC) and posterior capsular opacification (PCO), which is also known as ‘secondary cataract’, encompass the two major types of fibrotic cataracts, and are implicated by transforming growth factor-beta (TGF- β)-induced epithelial-to-mesenchymal transition (EMT) due to some form of ocular trauma (Eldred *et al.*, 2011).

ASC is a rare primary fibrotic cataract that forms just beneath the anterior lens capsule due to ocular trauma that include mechanical trauma, various inflammations and electrical burns (Figure 3) (Eldred *et al.*, 2011). An ASC forms when the monolayer of LECs, upon experiencing trauma, are stimulated to proliferate due to increased activation of inflammatory cytokines such as TGF- β (Hales, *et al.*, 1995). ASC pathogenesis progresses when LECs undergo EMT to transform into myofibroblasts that multilayer (Figure 3), express alpha-smooth muscle actin (α SMA), and produce ECM components such as collagens I and III and fibronectin that are not normally in a healthy ECM (Lee and Joo, 1999). The above processes lead to the formation of fibrotic plaques just beneath the anterior lens capsule, which result in light scattering and vision obstruction (Eldred *et al.*, 2011).

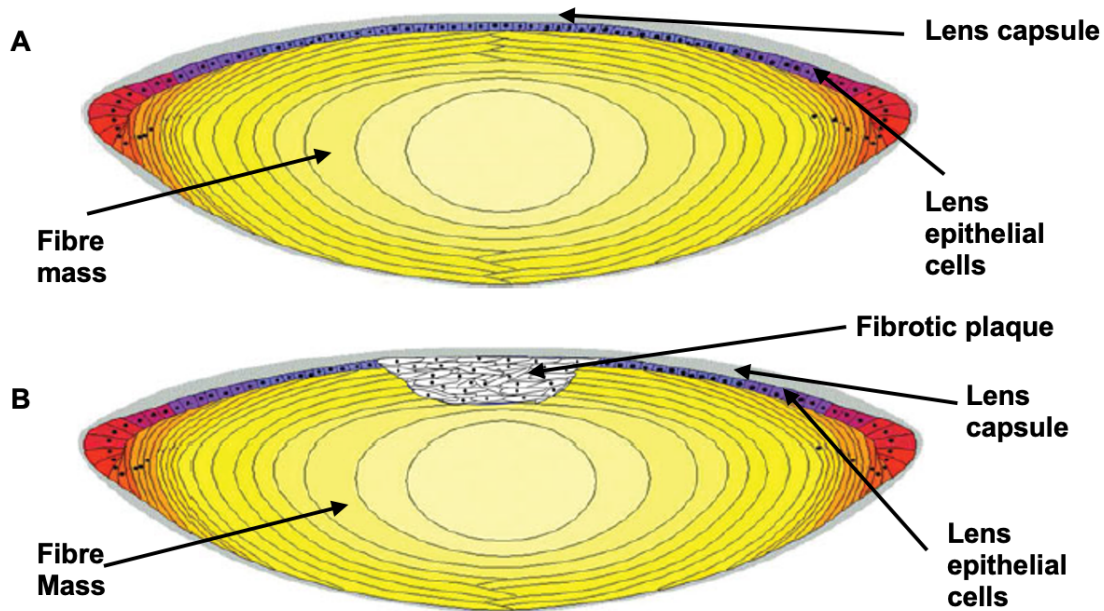


Figure 3. Anterior subcapsular cataract (ASC). A healthy lens (A) with an intact capsule (grey), a monolayer of LECs (red, pink and purple) and a fibre mass (orange and yellow). ASC is a primary cataract that involves the proliferation and elongation of LECs and is implicated by TGF- β -induced EMT (B). Adjacent LECs are recruited to the site of proliferation and will subsequently undergo EMT. These processes eventually lead to the formation of a fibrotic plaque (white) just beneath the anterior lens capsule. Figure adapted from Eldred *et al.*, 2011.

PCO is the most common post-cataract surgery complication in the world (Figure 4) (West-Mays and Sheardown, 2010). The ocular lens experiences tremendous stress during cataract surgery. Although most of the anterior lens capsule is removed during surgery, some persistent LECs are left behind on the remaining capsule in the germinative and transitional zones (Figure 4) (Wormstone, 2002) (Šikić *et al.*, 2017). The increased levels of active TGF- β trigger these cells to undergo EMT and transform into myofibroblasts (Kalluri and Weinburg, 2009). The three main steps to PCO formation include aberrant proliferation of LECs, migration to the posterior lens capsule and transformation into myofibroblasts (Wormstone, 2002) (Kalluri and Weinburg, 2009). These processes result in capsular wrinkling, excessive deposition of aberrant extracellular proteins and multilayering of cells at the posterior lens (West-Mays and Sheardown, 2010) (Wormstone, 2002). PCO risk increases in people who have undergone

cataract surgery at a younger age or experience chronic ocular inflammations (Batur *et al.*, 2016) (Eldred *et al.*, 2011). PCO is resolved by laser surgery, which is usually a safe procedure, but retinal detachment, macular edema, and corneal edema are potential side-effects (Billotte and Berdeaux, 2004).

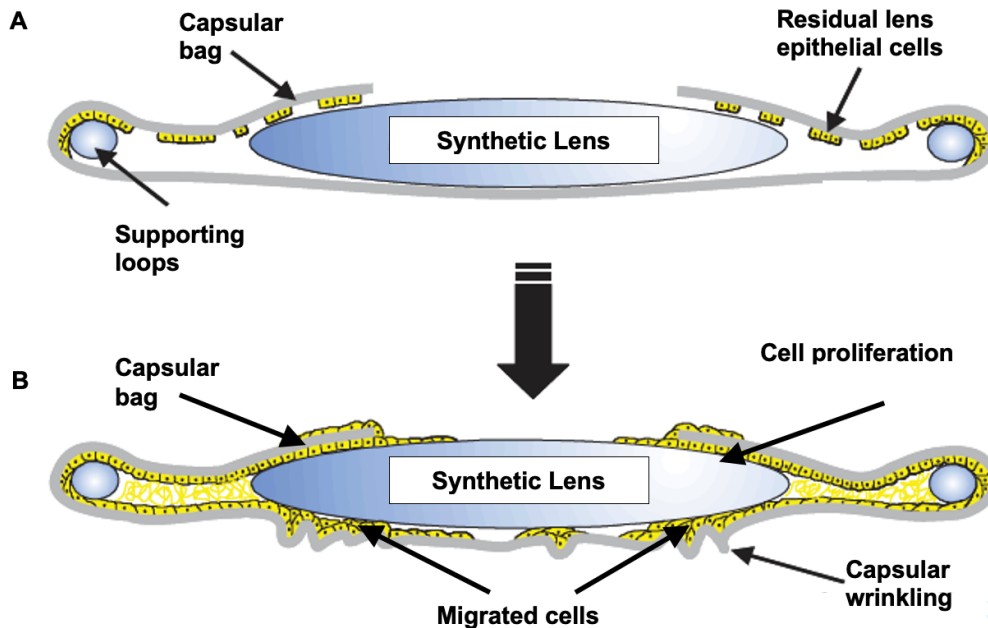


Figure 4. Posterior capsular opacification (PCO). The post-cataract surgery lens (A) consists of a capsular bag (grey) that is supported with loops and a synthetic lens. Residual LECs remain on the anterior capsule, and having experienced trauma, can undergo EMT. PCO occurs when the residual LECs have undergone EMT to proliferate, migrate from the anterior to the posterior capsule, and deposit excessive ECM components between the anterior and posterior capsules to cause posterior capsular wrinkling (B). PCO, which is also known as ‘secondary cataract’, is the leading complication of cataract surgeries. Figure adapted from Wormstone, 2002.

1.3 Fibrosis and the Lens as a Model for Fibrosis

Fibrosis occurs in a variety of tissues as myofibroblasts can arise from cells of epithelial or fibroblast origin (Kalluri and Weinburg, 2009). Thus, organs such as the kidneys, lungs, ocular lens, retina and serosal membranes are all vulnerable to fibrosis (Guarino *et al.*, 2009). Currently, the process of fibrosis cannot be reversed, but a greater understanding of the pathways

involved in this process can help define new targets and thus develop new therapeutics for fibrosis at different stages (Guarino *et al.*, 2009).

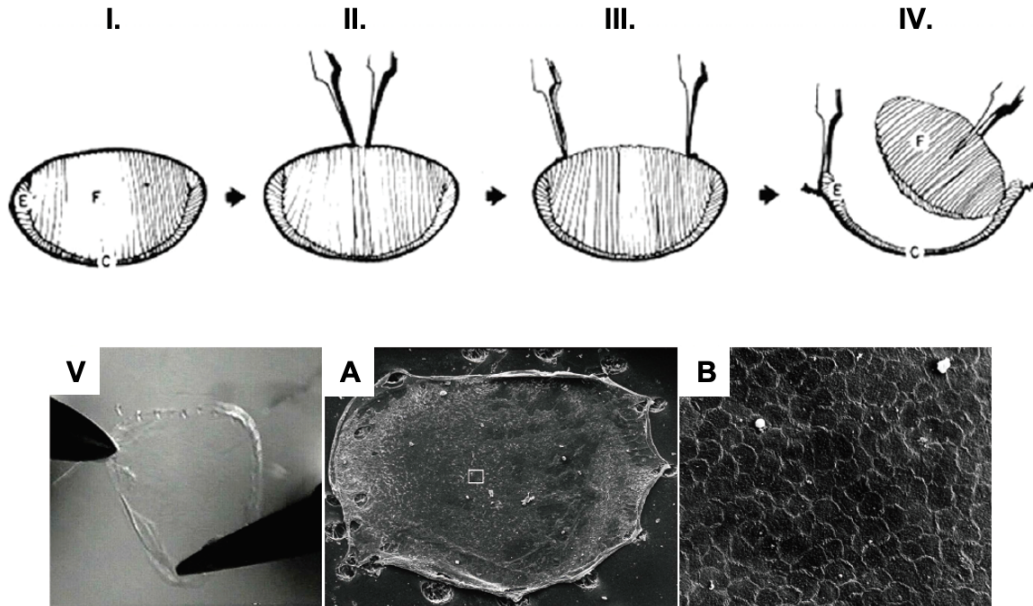


Figure 5. Lens epithelial cell explant protocol. E indicates epithelial cells, F indicates the fibre mass and C indicates the capsule. The lens is first isolated from rat pups that are 17-19 days old (I). The posterior capsule of the lens is pierced with fine forceps (II). The lens capsule is gently peeled toward the equator of the lens (III). The fibre mass is removed (IV) so that the epithelial cells remain on the anterior lens capsule. The explant is pinned down using a blunt tool (V). (A) shows a fully pinned lens epithelial explant. (B) shows the cuboidal lens epithelial cells with no treatment after 24 hours. Figure adapted from Korol, 2017.

The lens provides a unique model for studying EMT because it lacks blood vessels and innervation, and it is only made up of inactive fibre cells and LECs. As a result, any EMT that occurs can be attributed to an epithelial origin (Eldred *et al.*, 2011). Rat and mice LEC explants, which are primary cell explants, are ideal *ex vivo* models that our laboratory has employed. The explanting process involves the opening of the lens capsule from the posterior end and removing the fibre mass, followed by pinning of the entire anterior capsule with the LECs facing upwards (Figure 5I-V). If care is not taken during the last pinning step, the LECs on the explant can fall off the anterior capsule due to capsular stretching by the forceps. The LECs can also undergo

EMT without exogenous TGF- β treatment due to the mechanical stress experienced by the explant. Although the explanting process is difficult initially, this model offers many benefits once the technique is perfected. Since the explanted cells reside on their endogenous basement membrane, the *in vivo* situation of the cells can thus be recapitulated with *in vitro* methods (West-Mays *et al.*, 2010). In addition, viable primary LEC explants (Figure 5B) are not immortal, like commercially available LECs. This mortality of LEC explants is a benefit for studying TGF- β -induced EMT as cell immortality is a feature of cancer, and tumorigenesis is also another pathological process that is implicated by EMT (Kalluri and Weinberg, 2009).

1.4 TGF- β and Epithelial-to-Mesenchymal Transition

TGF- β is a group of multifunctional cytokines that play key roles in embryogenesis, cell differentiation, wound healing, adhesion and apoptosis (Miyazono, 2000). It is also a potent inducer of pathological conditions including fibrosis and cancer (Kalluri and Weinburg, 2009). The three isoforms of TGF- β in mammals, TGF- β 1-3, are well conserved among mammals (Lovicu *et al.*, 2016) and all three isoforms are present in the aqueous humour in their latent forms (Eldred *et al.*, 2011). TGF- β 1 and TGF- β 3 are both involved in wound healing responses and the subsequent activation of Smad proteins in the lung (Ask *et al.*, 2008). However, TGF- β 1 is associated with the pathological condition of progressive pulmonary fibrosis by inducing greater activations of TGF- β Receptors I and II, and by upregulating fibrosis-associated genes such as those for collagen I and fibronectin (Ask *et al.*, 2008). TGF- β 3 also seemed to play a regulatory role during TGF- β -induced pulmonary fibrosis as co-treatments with adenoviral deliveries of TGF- β 1 and TGF- β 3 seemed to prevent the upregulation of the TGF- β Receptors and the fibrotic ECM components (Ask *et al.*, 2008). TGF- β isoforms also have overlapping and distinct functions during lens fibrosis. Experiments using whole mouse lenses indicated a

requirement for Smad3 during TGF- β 2-induced lens fibrosis after a break was made in the anterior capsule of mouse lenses (Saika *et al.*, 2004). In addition, only TGF- β 2 was detected along the break made on the capsule (Saika *et al.*, 2004), suggesting the isoform's central role in inducing EMT after the lens suffers a capsular injury that is similar to cataract surgery. However, previous *in vivo* studies from our laboratory using transgenic mice overexpressing TGF- β 1 specifically in the lens revealed the development of ASC, and the plaque developed independent of Smad3 (Danh *et al.*, 2006). Furthermore, it was revealed that 0.025 ng/mL of TGF- β 2 or TGF- β 3 could induce capsular wrinkling in rat LEC explants, while 1 ng/mL of TGF- β 1 was required (Gordon-Thomson *et al.*, 1998). 0.05 ng/mL of TGF- β 2 or TGF- β 3 could also induce all three of the assessed responses: capsular wrinkling, cell elongation and cell-surface blebbing (Gordon-Thomson *et al.*, 1998). However, the lowest concentration of TGF- β 1 at which all three responses were induced was 1ng/mL (Gordon-Thomson *et al.*, 1998). The opacification index of whole rat lenses after treating with the three different isoforms of TGF- β was also assessed, and TGF- β 2 induced the highest levels of opacification at both of the tested concentrations (0.15ng/mL and 4 ng/mL) (Gordon-Thomson *et al.*, 1998). TGF- β 2 was thus used for the purposes of this thesis as TGF- β 2 is the predominant form in the aqueous humour that bathes the lens (Eldred *et al.*, 2011), and it also appeared to be the most potent inducer of lens fibrosis post-injury and in culture.

Endogenous mature TGF- β in the aqueous humour is a heterotetramer in its inactive latent form, and it consists of an active TGF- β homodimer attached to its latency-associated protein (LAP) homodimer (Yu and Stamenkovic, 2000) (Stockis *et al.*, 2009). Active TGF- β is tightly regulated by proteins such as α 2-macroglobulin in the aqueous humour, but active TGF- β is upregulated during a wound healing response after the lens experiences some form of trauma

(Eldred *et al.*, 2011). Activation of TGF- β involves the cleavage of the LAP by proteases such as plasmin, thrombospondin-1 and matrix metalloproteinases-2/9, integrin-mediated mechanisms, or by non-biological means such as heat, acid and reactive oxygen species (Figure 6) (Eldred *et al.*, 2011) (Yu and Stamenkovic, 2000). Active TGF- β binds to TGF- β Receptor I (TGF- β RI) that dimerizes with, and is phosphorylated by, the constitutively active TGF- β Receptor II (TGF- β RII) to initiate various intracellular pathways (Figure 6) (Miyazono, 2000). Disturbances in the negative regulation and termination of TGF- β signalling result in pathological conditions including fibrosis and cancer (Miyazono, 2000).

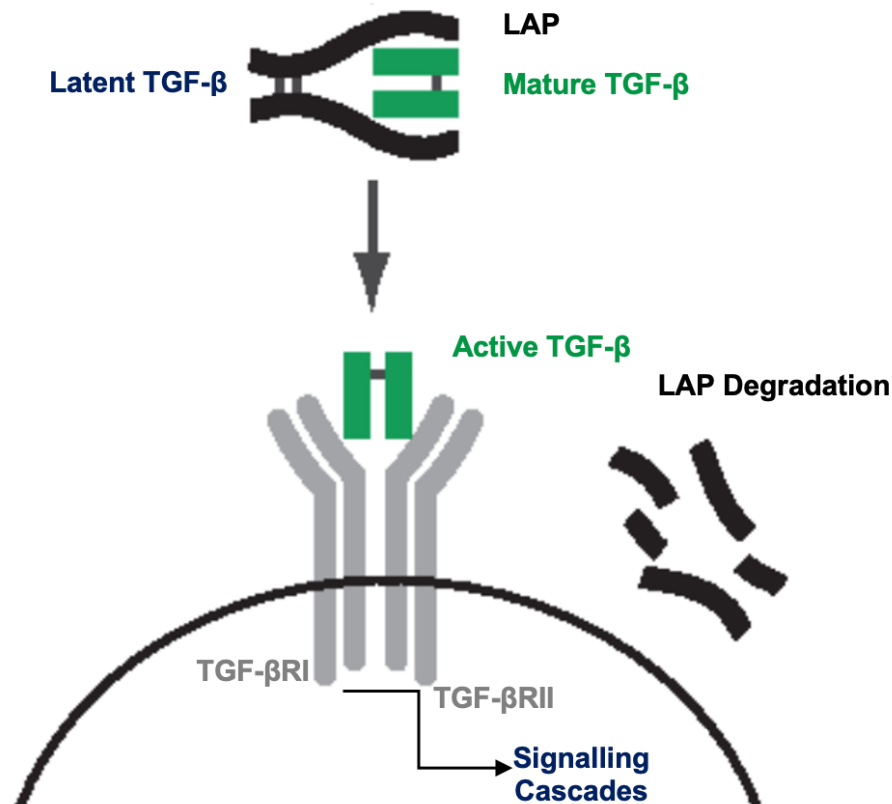


Figure 6. TGF- β activation. Endogenous TGF- β exist in its latent form, which consists of a homodimeric mature TGF- β and a homodimeric latency-associated protein (LAP). Upon activation, the LAP is cleaved and degraded, and mature TGF- β (green) is released. Active TGF- β binds to the TGF- β Receptors I and II dimer (TGF β RI and TGF β RII), which are serine/threonine kinases that activate intracellular signalling cascades. Figure adapted from Stockis *et al.*, 2009.

TGF- β activation under pathological conditions leads to epithelial-to-mesenchymal transition (EMT), a process that is central to fibrosis (Kalluri and Weinberg, 2009). EMT involves the transformation of cuboidal epithelial cells to mesenchymal myofibroblasts (Kalluri and Weinberg, 2009). Features of myofibroblasts include cell contractility, excessive deposition of fibrosis-associated extracellular matrix (ECM) components such as collagen I, collagen III, fibronectin and vitronectin, and formation of filamentous-actin (F-actin) and α SMA stress fibres (Figure 7) (Kalluri and Weinberg, 2009) (Eldred *et al.*, 2011). EMT is also associated with the loss of epithelial-cadherin (E-cadherin), which is the principal cell adhesion molecule (CAM) in LECs (Figure 6) (Kalluri and Weinberg, 2009).

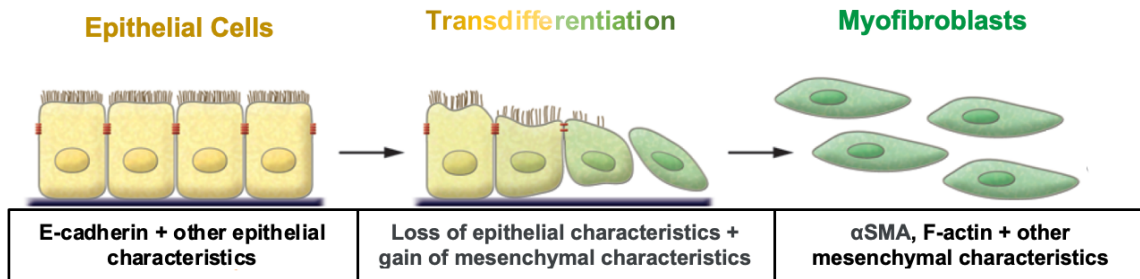


Figure 7. Epithelial-to-mesenchymal transition (EMT). TGF- β induced EMT involves the loss of epithelial characteristics such as E-cadherin, and the gain of mesenchymal characteristics such as α SMA. Figure adapted from Kalluri and Weinberg, 2009.

E-cadherin is connected to the actin-based cytoskeleton via the adheren junction protein, beta-catenin (β -catenin), and forms tight contacts between cells to hinder migration and maintain LECs in a contiguous sheet (Figure 8) (Cheng *et al.*, 2017) (Hay and Zuk, 1995). The loss of E-cadherin allows for migration and proliferation of LECs, and the delocalization of β -catenin from cell margins to the nucleus, where it acts as a nuclear transcription factor to further implicate EMT (Korol *et al.*, 2014). The ECM contributes to EMT progression via integrin-mediated mechanisms to enable cells to adhere and migrate across the ECM (Figure 9) (Guarino *et al.*,

2009). Of the many different types of integrins, integrin $\alpha 5 \beta 1$ is of particular interest for lens fibrosis because it and its ligand, fibronectin, are both upregulated by TGF- β signalling (Eldred *et al.*, 2011). In addition, integrin linked kinase (ILK), a serine/threonine kinase and regulator of ECM adhesion in LECs, binds to the cytoplasmic tail of the β chain of $\alpha 5 \beta 1$ and colocalizes with the integrin, especially in the presence of fibronectin (Weaver *et al.*, 2007). Increased ILK expression and the activation of the Wnt signalling pathway by TGF- β have been associated with EMT by inhibiting glycogen synthase kinase 3 beta (GSK-3 β) (Figure 9) (Guarino *et al.*, 2009). GSK-3 β is a key cytoplasmic protein that phosphorylates and inhibits cytoplasmic β -catenin and Snai1, both of which favor EMT (Figure 9) (Guarino *et al.*, 2009). The inhibition of GSK-3 β therefore results in cytoplasmic and nuclear accumulation of β -catenin (Figure 9), loss of E-cadherin and degradation of cell-to-cell junctions (Guarino *et al.*, 2009). $\alpha V \beta 5$ is another integrin of interest because it can be upregulated following mechanical trauma to allow for mechanotransduction signals from the extracellular microenvironments to influence LEC behaviour (Kass *et al.*, 2007). $\alpha V \beta 5$ plays a bi-directional role in LECs by perpetuating TGF- β activation and mediating mechanisms that cause EMT progression (Sponer *et al.*, 2005).

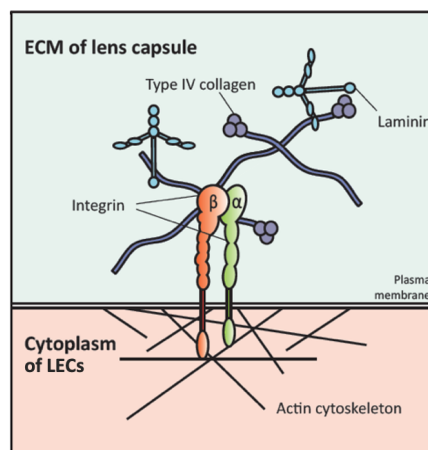


Figure 8. Attachment of LECs to the lens capsule. The ECM of the lens capsule consists of a meshwork of collagen IV (purple) and laminin (blue). The LECs have protruding integrins made up of β and α chains that connect the ECM to the actin cytoskeleton in the cytoplasm. Figure adapted from West-Mays and Korol, 2014.

TGF- β induced fibrosis proceeds via Smad-dependent and Smad-independent pathways (Hu *et al.*, 2018). The most characterized TGF- β signalling pathway is the canonical Smad pathway, which involves three subclasses of Smads: receptor regulated Smads (R-Smads), Common Partner Smads (Co-Smads) and Inhibitory Smads (I-Smads) (Miyazono, 2000). Smad2 and Smad3 are specific R-Smads of TGF- β induced pathways in mammals, and they are directly phosphorylated by TGF- β RI (Figure 9) (Guarino *et al.*, 2009) (Miyazono, 2000). Phosphorylated Smad2/3 binds with the only mammalian Co-Smad, Smad4, to form the R-Smad-Smad4 complex, which translocates from the cytoplasm to the nucleus of the cell and remains there for several hours post-translocation to act as a transcription factor to upregulate the expression of EMT-associated genes (Figure 9) (Guarino *et al.*, 2009) (Miyazono, 2000). TGF- β induced Smad-independent pathways include the p38, ERK1/2, PI3K and Rho/Rho-associated protein kinase (ROCK) pathways (Hu *et al.*, 2018) (Guarino *et al.*, 2009). However, such pathways have been shown to interact with Smad-dependent pathways in the lens (Taiyab *et al.*, 2019).

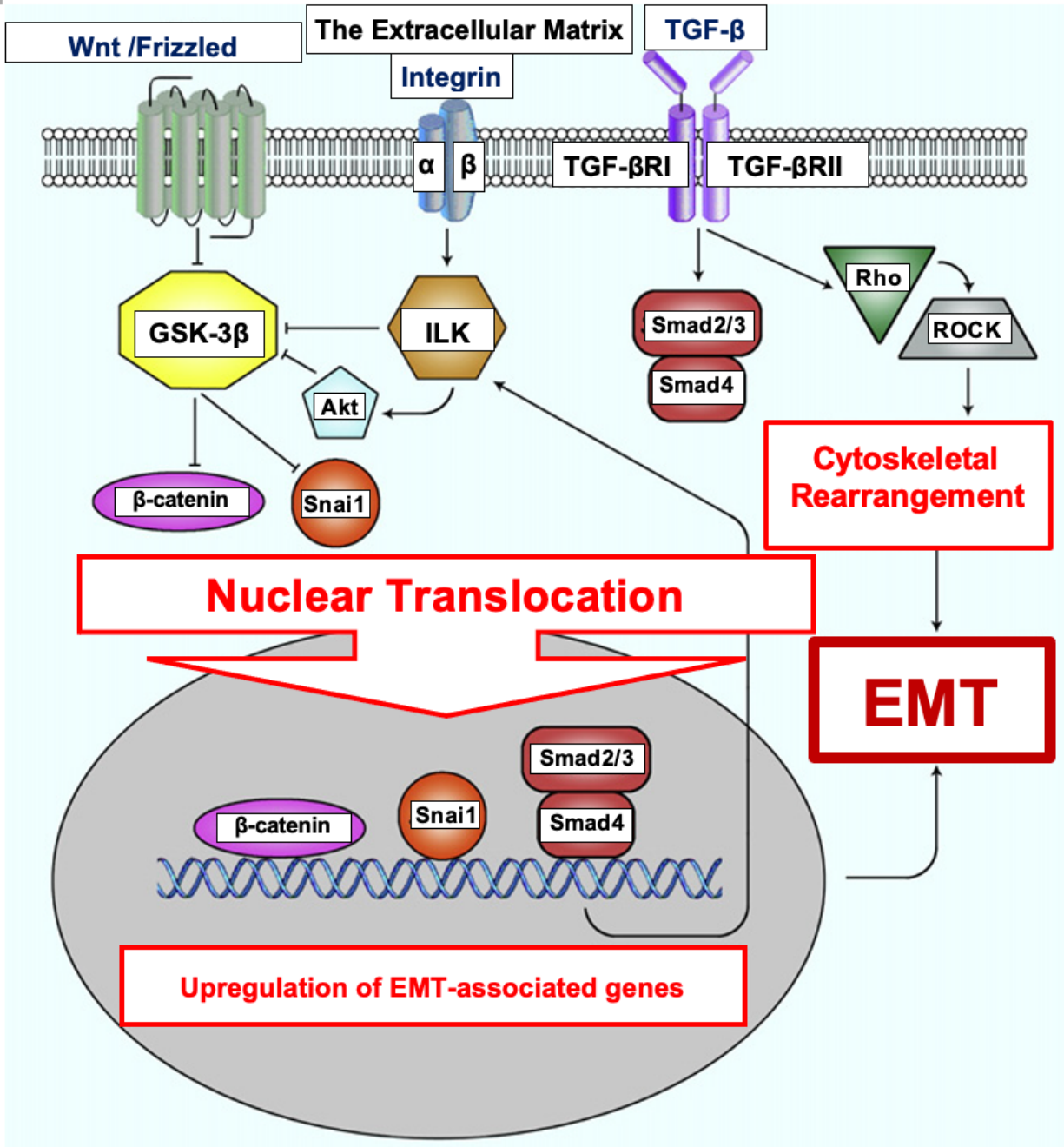


Figure 9. Major TGF- β induced signalling pathways involved in EMT. TGF- β can induce cellular via 3 major types of cell surface receptors: Wnt/Frizzled, integrin and TGF- β . Wnt signalling ultimately results in the inhibition of GSK-3 β , which reduces GSK-3 β 's inhibition on cytoplasmic β -catenin and Snai1. β -catenin and Snai1 can both translocate to the nucleus to upregulate EMT-associated genes. Integrin-extracellular matrix interactions can activate ILK, which can directly and indirectly inhibit GSK-3 β via Akt. The canonical Smad pathway is mediated by TGF- β receptors (TGF- β R) TGF- β receptors also mediate the Rho/ROCK pathway that causes cytoskeletal rearrangement and lead to EMT. Figure adapted from Guarino *et al.*, 2009.

1.5 Matrix Metalloproteinases and Cytoskeletal Modifications

Matrix Metalloproteinases (MMPs) are a family of zinc-dependent proteases that degrade the ECM, and are involved in processes such as embryogenesis, wound healing and fibrosis (Stamenkovic, 2003). MMP2 and MMP9 are associated with TGF- β induced EMT because they can activate latent TGF- β in the aqueous humour, and active TGF- β can in turn upregulate MMP2 and MMP9 (Yu and Stamenkovic, 2000). In addition, MMP2 and MMP9 can degrade collagen IV of the lens capsule, and collagen IV is replaced with an excessive amount of fibrotic ECM proteins that cannot be regulated (Chakraborti *et al.*, 2003) (Eldred *et al.*, 2011). Our laboratory has shown that co-treatment of GM60001 (a broad MMP inhibitor) or a MMP2/9-specific inhibitor and TGF- β 2 reduced EMT and ASC in the ocular lens (Dwivedi *et al.*, 2006). Additional knock-out (KO) studies from our laboratory demonstrated that MMP9 is essential for TGF- β -induced EMT and may play an essential role in cytoskeletal remodelling during EMT (Korol *et al.*, 2014). MMP9KO and MMP2KO mice were developed as *in vivo* models, and were subjected to two different TGF- β sources: the first is the use of adenoviral gene transfers of TGF- β 1 to the anterior segment of the eye that provided a relatively transient source of TGF- β 1, and the second is breeding KO mice with a lens-specific TGF- β 1 overexpression model (TG:MMP9KO), where the lens was exposed to active TGF- β 1 since development (Korol *et al.*, 2014). In the more transient TGF- β 1 adenoviral gene transfer model, MMP9KO mice demonstrated a lack of cell proliferation and α SMA expression similar to that of wildtype untreated controls, whereas MMP2KO demonstrated cell proliferation and α SMA expression similar to that of wildtype mice that received the adenoviral delivery of TGF- β 1 (Korol *et al.*, 2014). However, studies using the TG:MMP9KO mouse model demonstrated that the lack of MMP9 inhibited EMT in 75% of the cases, and conferred resistance in 25% of the cases (Korol

et al., 2014). Therefore, MMP9 deficiency is not sufficient to inhibit EMT entirely on its own upon chronic TGF- β exposure but did offer resistance against EMT in all cases (Korol *et al.*, 2014). In order to validate the findings found using the *in vivo* models, our laboratory used *ex vivo* mice LEC explants from wildtype, MMP9KO and MMP2KO mice to assess α SMA, E-cadherin and β -catenin localization via immunofluorescence staining (Korol *et al.*, 2014).

Untreated and TGF- β 2 treated MMP9KO LECs demonstrated no expression of α SMA, which were comparable to that of untreated wild-type controls. In addition, E-cadherin were localized to the cell margins and the cuboidal shape of LECs were retained in untreated and TGF- β 2 treated MMP9KO LECs. Furthermore, immunofluorescence staining of untreated and TGF- β 2 treated MMP9KO LECs demonstrated the localization of β -catenin to cell margins and retainment of cuboidal LEC shape and were comparable to that of the untreated wildtype LECs. Therefore, MMP9 deficiency seemed to inhibit β -catenin nuclear translocation, which was observed in the TGF- β treated wildtype LECs. Alterations to the LEC cytoskeleton that were observed in MMP9KO LECs were not observed in MMP2KO LECs (Korol *et al.*, 2014).

1.6 Actin Polymerization and Cytoskeletal Remodelling During TGF- β -induced EMT

The Rho family of GTPases is responsible for the regulation of actin-based structures in the cytoskeleton of epithelial cells, and ROCK upregulates the phosphorylation of myosin light chain (MLC) to stimulate actin-myosin filament assembly and cytoskeletal remodelling (Figure 9) (Guarino *et al.*, 2009). The Rho/ROCK pathway will consequently lead to increased F-actin stress fibres, which contribute to cellular contractility, migration and change of cellular shape from cuboidal LECs to elongated myofibroblasts (Haynes *et al.*, 2011). The increase in F-actin polymerization leads to a cellular decrease in the concentration of actin subunits and globular actin (G-actin). The MRTF-A/G-actin complex thus dissociates to provide additional G-actin to

be added to the growing F-actin stress fibres (Olson and Nordheim, 2010) (Yu *et al.*, 2014).

Upon dissociation, free MRTF-A translocates to the nucleus to act as a transcription factor to further implicate TGF- β -induced EMT in the lens, kidney, lungs and heart (Gupta *et al.*, 2013) (Korol *et al.*, 2016) (O'Connor *et al.*, 2015) (Zhou *et al.*, 2013) (Small, 2012). Our laboratory has previously shown that inhibition of the Rho/ROCK pathway prevented TGF- β -induced EMT, where rat LECs co-treated with TGF- β and a ROCK inhibitor (Y-27632) demonstrated similar phosphomyosin and F-actin immunofluorescence staining patterns as untreated rat LECs (Korol *et al.*, 2016).

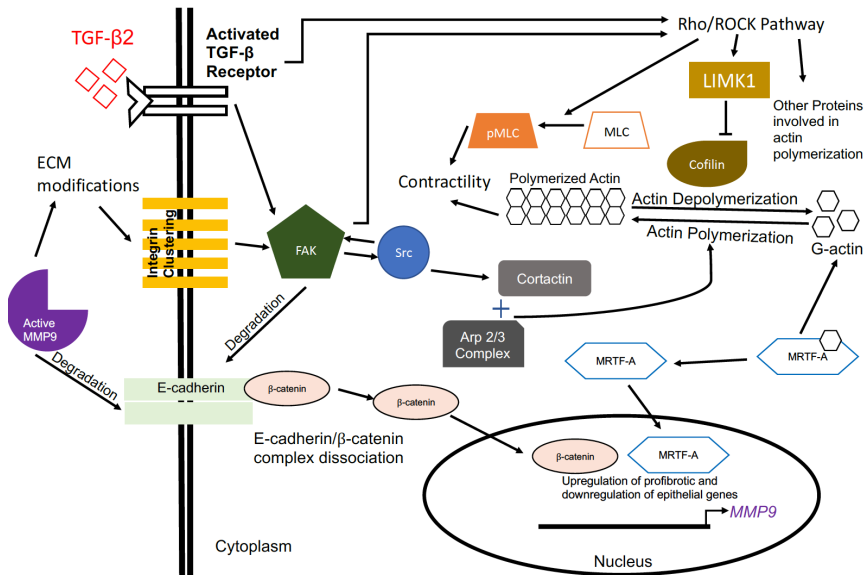


Figure 10. Simplified summary of potential actin polymerization pathways during TGF- β 2 induced EMT. Active MMP9 could cause E-cadherin and collagen IV degradation. E-cadherin dissolution allows β -catenin to translocate to the nucleus to upregulate EMT-associated genes. Collagen IV is replaced by fibrosis-associated ECM components, and changes to the ECM can result in integrin clustering. FAK activation could occur via activated TGF- β receptors and integrin clustering. Upon phosphorylation of FAK at Tyr397, Src is also phosphorylated and activated. Src could phosphorylate other tyrosine phosphorylation sites on FAK and cortactin to promote actin polymerization. Activated FAK could activate the Rho/ROCK pathway, which could lead to the activation LIMK1, phosphorylation of MLC and activation of other proteins involved in actin polymerization. Activated LIMK1 phosphorylates and therefore inhibits cofilin's actin depolymerization activity. Phosphorylated MLC form complexes with polymerized actin to cause cell contractility. G-actin monomer shortage caused by increased actin polymerization induces the dissociation of G-actin from MRTF-A, allowing MRTF-A to translocate to the nucleus to further implicate EMT.

There are also other proteins and pathways that could contribute to cytoskeletal remodelling during TGF- β -induced EMT (Figure 10). For instance, cortactin, a multidomain protein, is involved in actin assembly and maintenance, and it is activated by tyrosine kinases such as Src at Tyr 421, Tyr466 and Tyr482 (Daly, 2004). Cortactin acts to protect newly polymerized F-actin by binding to newly added ATP or ADP-Pi subunits, whereas cofilin, an actin depolymerizing protein, binds to older ADP subunits (Bamburg and Bernstein, 2010). In addition, cortactin binds to and activates the actin related protein (Arp) 2/3 complex, which is essential for driving actin nucleation, branching and polymerization (Daly, 2004) (Bamburg and Bernstein, 2010) (Weed *et al.*, 2000). Furthermore, the co-localization of cortactin with cortical F-actin is associated with cell migration, which is a characteristic of the myofibroblasts in PCO (Daly, 2004) (Eldred *et al.*, 2011).

When the cells experience mechanical stress, integrins, which connect the cellular actin cytoskeleton with the ECM, become activated (Figure 10) (Lee and Nelson, 2012). The activation of integrins result in integrin-clustering, and this process promotes the activation of FAK. Activated FAK mediates many intracellular signalling pathways of the mechanotransduction cascade (Lee and Nelson, 2012). FAK is a major component of focal adhesion complexes, where it co-localizes with and phosphorylates other FAC components including paxillin, vinculin and talin (Grigera *et al.*, 2005) (Lee and Nelson, 2012). The activation of FAK involves the autophosphorylation at Tyr397 (Grigera *et al.*, 2005), which leads to the activation of Src and Src family kinases, and activated Src can in turn phosphorylate FAK at other tyrosine sites (Lee and Nelson, 2012). Src phosphorylation of FAK leads to the binding of FAK to proteins with SH3 domains, including the Rho GTPase-activating proteins (GAPs) and GTP exchange factors (GEFs) to stimulate the Rho-family GTPases including RhoA, Rac

and CDC42 which mediate stress fibre, lamellipodia and filopodia formations respectively (Mitra *et al.*, 2005) (Schwock and Dhani, 2011). In addition, FAK activation also promotes cell contractility and cell migration via two pathways that ultimately result in the phosphorylation of MLC (Lee and Nelson, 2012). First, FAK's bindings to GAPs and GEFs activate the previously mentioned Rho/ROCK pathway (Lee and Nelson, 2012). The activation of FAK also leads to the stimulation of the Grb2/Ras/Raf/MEK/ERK pathway, and phosphorylated ERK activates myosin light chain kinase (MLCK), leading to increased phosphorylation of MLC (Lee and Nelson, 2012). The induction of the Ras/Raf/MEK/ERK pathway also leads to the upregulation of EMT-associated genes such as those associated with cell proliferation, differentiation and ECM remodelling (Grigera *et al.*, 2005) (Lee and Nelson, 2012). The activation of Rho and Grb2 by FAK can also lead to microtubule, another cytoskeletal component, stabilization by interacting with mDia and dynamin respectively (Schwock and Dhani, 2011). In addition, studies have also shown that during TGF- β -induced EMT, Src/FAK signalling regulates E-cadherin degradation and delocalization (Figure 10) (Cicchini *et al.*, 2008). Upon longer stimulation with TGF- β , the Src/FAK signalling pathway was also found to downregulate the transcription of E-cadherin (Cicchini *et al.*, 2008).

Lim-domain kinase-1 (LIMK1) is a crucial regulator of actin dynamics by phosphorylating and inhibiting the key actin-binding and depolymerizing protein, cofilin (Prunier *et al.*, 2017). It also regulates microtubule dynamics by promoting microtubule depolymerization into tubulin dimers (Prunier *et al.*, 2017). LIMK1 is activated by serine/threonine kinases at Thr508 by tyrosine kinase induced pathways, including the TGF- β -induced Rho/ROCK and Rac/CDC42/PAK pathways (Scott and Olsen, 2007) (Chen *et al.*, 2019) (Ohashi *et al.*, 2000). Research has also shown that the downregulation of LIMK1 reduced actin

polymerization and fibronectin secretion in corneal fibroblasts (Gorovoy *et al.*, 2008), which could mean that the protein also has a role during TGF- β -induced EMT in the lens.

1.7 The actin polymerization machinery may be inactive due to the lack of MMP9

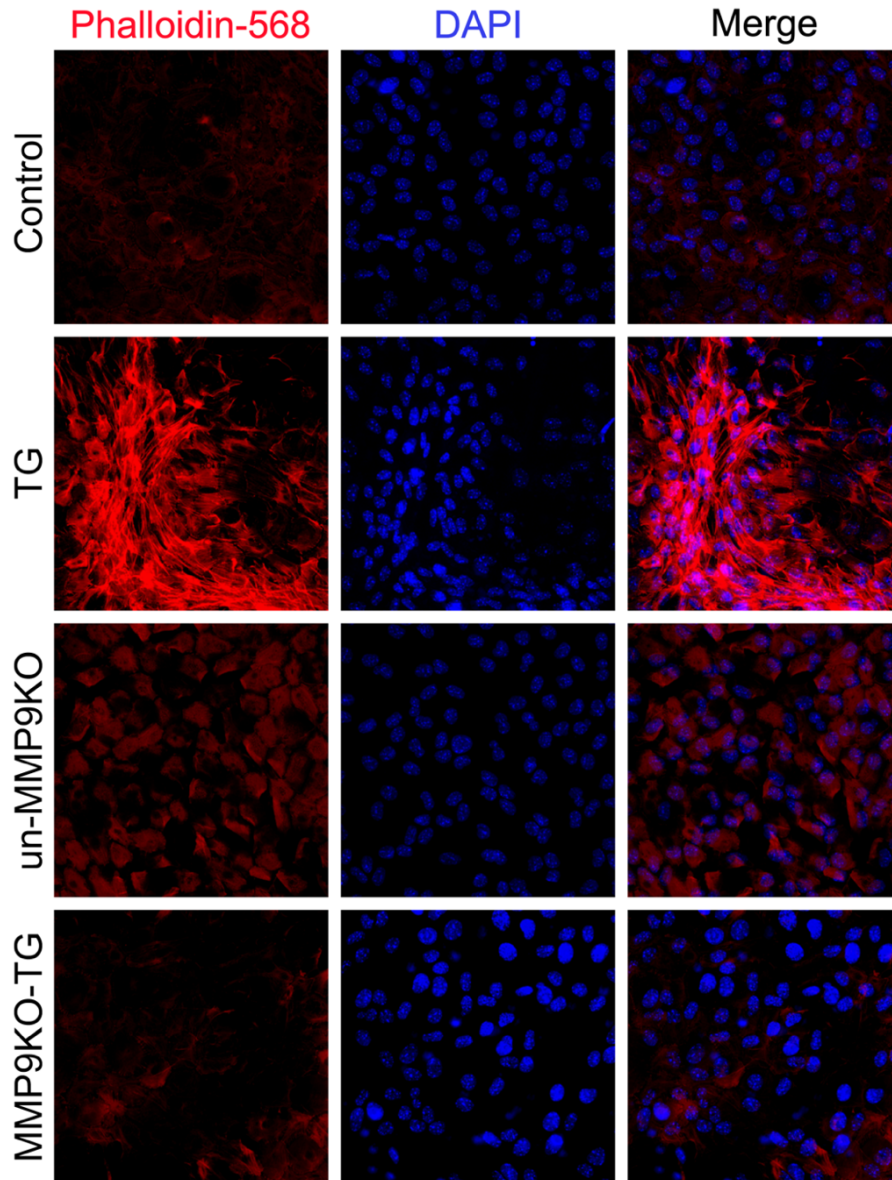


Figure 11. Phalloidin staining for F-actin. LEC explants from wildtype mice were left untreated (control) or treated with 500pg/mL TGF- β for 72 hours (TG) ($n = 3$ experiments where $n \geq 3$ explants per treatment were used for each experiment). LEC explants from MMP9KO mice were left untreated (un-MMP9KO) or treated with 500pg/mL TGF- β for 72 hours (MMP9KO-TG) ($n = 3$ experiments where $n \geq 3$ explants per treatment were used for each experiment). Paraformaldehyde (PFA) fixed explants were stained for F-actin using phalloidin-568. Images were acquired using Leica DM6 fluorescence microscope at 40X. Experiment performed by Dr. Aftab Taiyab (unpublished).

Our laboratory has previously shown that TGF- β 2 treated LECs from MMP9KO mouse eyes were unable to polymerize α SMA (Korol *et al.*, 2014). In addition, absence of MMP9 has been correlated with a lack of F-actin in astrocytes (Hsu *et al.*, 2008). Our laboratory therefore examined if F-actin formation is also defective in MMP9KO LECs upon TGF- β treatment. Indeed, a staining with phalloidin showed an absence of F-actin in the TGF- β treated MMP9KO LECs when compared to TGF- β treated wildtype LECs (Figure 11) (unpublished data). The next step was to determine if the lack of α SMA and F-actin polymerization was due to a deficiency in gene or protein expression of actin. In order to determine whether MMP9 plays a role in regulating the gene expression of actin, a Nanostring analysis was performed to quantify the number of mRNA transcripts for α SMA (*ACTA2*) and β -actin (*ACTB*). Lenses from wildtype mice, transgenic mice overexpressing TGF- β 1 (TGF β ^{tg}) in the lens and TGF β ^{tg} on the MMP9KO background (TG:MMP9KO) were used to perform the experiment four times (Figure 12) (unpublished data). Our MMP9KO mice could potentially express the mRNA for MMP9, but the mRNA codes for a defective protein as part of exon 2 and all of intron 2 of the *MMP9* gene were replaced with a *pgk-neo* gene cassette (Korol *et al.*, 2014). Therefore, in order to ensure that our transgenic TG:MMP9KO mouse model was functional, *MMP9* expression was also analyzed as a positive control during the NanoString analysis because TGF- β is known to upregulate *MMP9* expression (Nathu *et al.*, 2009). A 12-fold upregulation of *MMP9* expression was observed in TGF β ^{tg} LECs when compared to wildtype LECs (Figure 12A; **** $p < 0.0001$). Furthermore, a 150-fold increase in *MMP9* expression was observed in the TG:MMP9KO versus wildtype LECs when compared to a 13-fold increase in *MMP9* expression between TG:MMP9KO and TGF β ^{tg} LECs (Figure 12A; **** $p < 0.0001$). There was a significant 1.5-fold increase in α SMA (*ACTA2*) expression in TGF β ^{tg} LECs (1.55 ± 0.01) and TG:MMP9KO LECs (1.54 ± 0.01) when

compared to wildtype LECs (1.01 ± 0.01) (Figure 12B; **** $p < 0.0001$). However, *ACTA2* levels were not significantly different between TGF β^{tg} and TG:MMP9KO LECs (Figure 12B; $p = 0.55$). In addition, there was no marked difference in β -actin gene expression (*ACTB*) between wildtype and TGF β^{tg} LECs (Figure 12C; *** $p < 0.001$), and between wildtype and TG:MMP9KO LECs (Figure 12C; **** $p < 0.0001$). *ACTB* expression was also not notably different between TGF β^{tg} and TG:MMP9KO LECs (Figure 12C; * $p < 0.05$). Although α SMA or F-actin polymerization were not observed in MMP9KO mouse LECs that were stimulated with an exogenous source of TGF- β (Korol *et al.*, 2014) (Figure 11), no marked difference was observed in *ACTA2* and *ACTB* expression between TGF β^{tg} and TG:MMP9KO mouse LECs (Figures 12B and C). Hence, it was surmised that components of the actin polymerization machinery may be inactive as a result of the lack of MMP9.

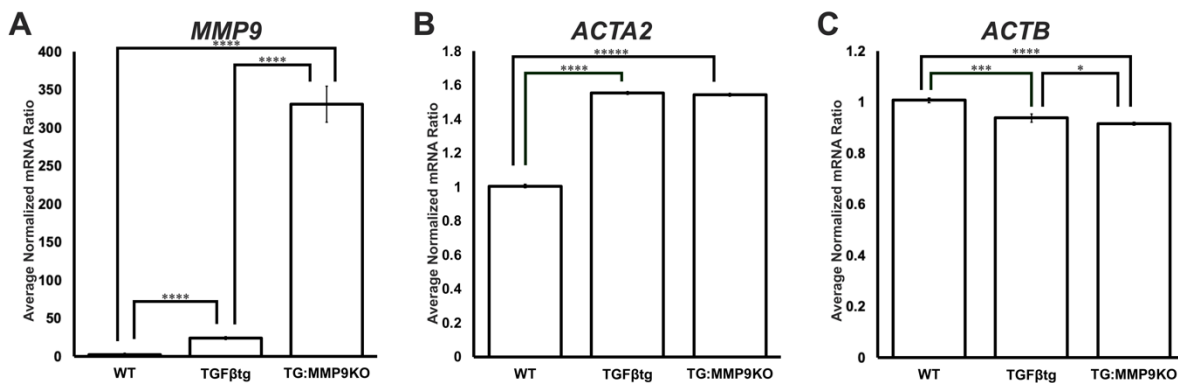


Figure 12. Expression of *MMP9* (A), *ACTA2* (B), and *ACTB* (C) during NanoString analysis. Lenses were obtained from wildtype (WT) ($n = 4$ experiments, where $n = 3$ lenses per experiment), TGF- β overexpressing (TGF β^{tg}) ($n = 4$ experiments, where $n = 3$ lenses per experiment) and TGF β^{tg} on the MMP9KO background (TG:MMP9KO) ($n = 4$ experiments, where $n = 3$ lenses per experiment) mice. The NanoString nCounter gene expression system was used to quantify the expression of *MMP9* (A), *ACTA2* (B) and *ACTB* (C). The data was normalized to total RNA count, and the normalized mRNA ratios were calculated by referencing to one set of WT. Error bars indicate \pm standard deviation of the average normalized mRNA ratios (* $p < 0.05$; *** $p < 0.001$; **** $p < 0.0001$). Experiment performed by Dr. Aftab Taiyab (unpublished).

To demonstrate the role of MMP9 in modulating the expression and activation of proteins required during actin polymerization and reorganization, a cytoskeletal protein array (Fullmoon Biosystems) was performed using untreated and TGF- β 2-treated wildtype and MMP9KO mouse LECs (unpublished data). Numerous proteins were observed to be differentially expressed and phosphorylated upon TGF- β 2 stimulation between wildtype LECs and MMP9KO LECs (Figure 13). In particular, nine proteins were upregulated by 1.26 to 3.11-fold in TGF- β 2-treated wildtype LECs (TG) when compared to untreated wildtype mouse LECs (control), but similar levels of upregulation were observed between TGF- β 2-treated MMP9KO (MMP9KO-TG) and untreated MMP9KO (un-MMP9KO) mouse LECs (Figure 13).

Actin polymerization and cytoskeletal remodelling during TGF- β -induced EMT involves a myriad of proteins that work in synergy. Overall, our laboratory has discovered that the cytoskeleton is modified in the LECs of MMP9KO mice (Korol *et al.*, 2014), and investigations into F-actin polymerization, actin gene expression and protein expression have revealed that the actin polymerization machinery may be defective. This thesis will thus focus on investigating the effects of MMP9 deficiency on the expression and activation of selected proteins from the protein array to reveal cytoskeletal remodelling pathways that may be regulated by MMP9.

Antibody List	Fold Change Between Samples	
	TG/control	MMP9KO-TG/un-MMP9KO
Cofilin (Ab-S3)	2.27	0.93
Cortactin (Ab-Y466)	3.11	0.80
FAK (Ab-Y910)	2.34	1.03
FAK (Ab-pY861)	1.27	0.71
Filamin A (Ab-S2152)	1.59	1.16
LIMK1 (Ab-T508)	2.85	1.08
LIMK1 (Ab-pT508)	1.26	1.17
MLC2 (Ab-S18)	1.74	1.06
MLC2 (Ab-pS18)	1.57	0.72
Rac1/CDC42 (Ab-S71)	1.28	0.76
Rho/Rac guanine nucleotide exchange factor (Ab-pS885)	1.31	1.22
VASP (Ab-157)	2.08	1.11

Figure 13. Notable fold changes from the cytoskeletal protein array. Cytoskeletal protein array analysis was conducted using untreated wildtype (control), 500 pg/mL TGF- β 2 treated wildtype for 72 hours (TG), untreated MMP9KO (un-MMP9KO) and 500pg/mL TGF- β treated MMP9KO for 72 hours (MMP9KO-TG) mouse LEC explants. The experiment was conducted 3 times, and 10 μ g of protein per treatment was used for each experiment. Red represents upregulation, green represents downregulation and white represents no notable difference was observed between the two compared treatment groups. A darker shade of the color of the box indicates a greater fold difference between the two compared treatment groups. Experiment performed by Dr. Aftab Taiyab (unpublished).

CHAPTER TWO

Main Hypothesis and Specific Aims

2.1 Main Hypothesis

MMP9 plays a role in regulating proteins involved in actin polymerization and cell migration during TGF- β 2 mediated EMT in the ocular lens.

2.2 Specific Aims

Aim 1: Validate the MMP9-specific inhibitor, JNJ0966, for use in rat LEC explants.

Previously available MMP9-specific inhibitors function by blocking the active site of MMP9. MMP9 has 56-64% homology with other MMPs at the catalytic domain (Massova *et al.*, 1997). In addition, as gelatinases, MMP9 share many substrates with MMP2, including collagen IV, elastin, and vitronectin (Vu, 2001). As a result of these homologies, cross inhibition with other MMPs could occur with inhibitors that target the catalytic domain or the active site.

JNJ0966 was discovered as a novel inhibitor that prevents the activation of MMP9 by inhibiting an allosteric site (Scannevin *et al.*, 2017). This inhibitor has also been shown to inhibit EMT associated gastric tumorigenesis (Liu *et al.*, 2019), but its efficacy in fibrotic models or in the lens has yet to be tested.

The previous MMP9 deficient model that was employed by our laboratory was MMP9KO mice. However, due to the larger size of rat LEC explants to mouse explants, rat explants can offer more protein per explant for conducting protein expression analyses such as western blots. In addition, the use of rat LECs with this inhibitor can also increase the efficiency of experiments as resources and time could be saved from housing and breeding transgenic animals, but as outlined under 1.3, the *in vivo* situation of cells could still be recapitulated in these primary explants. Immunofluorescence staining for α SMA and E-cadherin will be conducted to investigate the efficacy of JNJ0966 in preventing TGF- β 2-induced EMT in rat LEC explants.

Aim 2: Identify MMP9-dependent signalling molecules in stress fibre formation of TGF- β 2-induced EMT in the lens.

Earlier findings from our laboratory revealed a lack of F-actin polymerization, despite normal levels of actin monomer expression. Differential regulation of cytoskeletal proteins in the MMP9KO mouse LECs was shown by the protein array. Therefore, the next step is to validate the protein array results by selecting molecules and revealing their expression and localization in MMP9-deficient models via western blot and immunofluorescence analyses. Proteins will be selected based on a fold change of 1.5 or greater between TGF- β 2 treated and untreated wildtype mouse and their central roles in actin polymerization and dynamics (Figure 10). This aim will be completed using untreated or TGF- β 2 treated rat LECs that will be co-treated or not with the MMP9-specific inhibitor, JNJ0966.

Aim 3: Reveal MMP9-dependent pathways that result in cytoskeletal modification during TGF- β -induced EMT of the lens.

MRTF-A is a master regulator of TGF- β induced EMT, and its dissociation from G-actin, and subsequent translocation to the nucleus is affected by increased actin polymerization (Gupta *et al.*, 2013). The dissociation of MRTF-A from G-actin is a process that is downstream of stress fibre formation and maintenance, which are implicated by Rho/ROCK signalling. Therefore, an understanding of the localization of MRTF-A upon MMP9 inhibition can further elucidate the role of Rho/ROCK signalling in TGF- β induced EMT in the lens. Immunofluorescence staining for MRTF-A will be conducted using rat LECs and the MMP9-specific inhibitor, JNJ0966.

CHAPTER THREE
Materials and Methods

3.1 Obtaining and Culturing *ex vivo* rat LEC explants

All animal studies were performed according to the Canadian Council on Animal Care Guidelines and approved by McMaster's Animals Research Ethics Board. As a primary explant, the culture media must be supplemented with antibiotics that cover a broad spectrum of potential contaminating microbes including gram positive and negative bacteria, mycoplasma, fungi and yeast ("Why Use Antibiotics in Cell Culture?", n.d.). Serum-free M199 media was supplemented with penicillin-streptomycin, Amphotericin B and gentamicin for culturing the explants; all of the above reagents were purchased from Gibco by Life Technologies. 17-19 days old rat pups were euthanized using carbon dioxide (CO₂) followed by cervical dislocation. Whole eyes were removed using curved scissors and placed in a 35mm polystyrene tissue culture dish containing prewarmed (37°C) media. The posterior of the eye was located, and the lenses were removed by gently tearing open the eye from the posterior side, and all other ocular structures are discarded. The lenses were transferred to new culture dishes containing fresh and prewarmed (37°C) media, and the LEC explant containing the intact anterior capsule with LECs was isolated by peeling open the capsule from the posterior end and discarding the fibre mass. The explant was then pinned down using a blunt tool with the LECs facing up to be bathed by the medium. The explants were incubated at 37°C at 5% CO₂ and 95% humidity overnight and examined for viability the next day.

3.2 Treatments of Rat LEC Explants with TGF-β₂ and JNJ0966

Rat LEC explants were treated with <0.5% of DMSO, 6-10 ng/mL of recombinant human TGF-β₂ (R&D Systems, Minneapolis, MN, USA) for 48 hours, 20μM of JNJ0966 (Tocris) for 48 hours or pretreated for 2 hours with 10-20μM JNJ0966 and then treated with 6-10ng/mL of

recombinant human TGF- β 2 (R&D Systems, Minneapolis, MN, USA) for 48 hours in 2mL of media.

3.3 Immunofluorescence Staining

Explants were fixed following treatment using 4% paraformaldehyde (PFA) at room temperature for 10-12 minutes and washed using phosphate buffered saline (PBS). Explants were then lifted from the plates and transferred to separate glass test tubes with PBS. PBS was then removed, and the explants were incubated with permeabilizer (0.1% Triton X-100, 0.5% sodium dodecyl sulphate in PBS) and blocked with 5% normal donkey serum (Invitrogen) for 1 hour at room temperature. Explants are then incubated with primary antibodies at 1:200 dilution overnight at 4°C. Primary antibodies included those for FAK (Abcam Inc.), E-cadherin, phosphorylated FAK at Tyr397, LIMK1, phosphorylated LIMK1 at Thr508 and cortactin (Invitrogen), phosphorylated MLC2 at Ser18 (Millipore Sigma) and MRTF-A (Santa Cruz Biotechnology). Explants were washed three times with PBS for 10 minutes per wash and incubated with secondary antibodies at 1:200 dilution for 1 hour at room temperature to visualize unconjugated primary antibodies. Secondary antibodies were obtained from Thermo Fischer Scientific and included donkey anti-rabbit antibodies conjugated to Alexa Fluor®568, donkey anti-rabbit antibodies conjugated to Alexa Fluor®488, donkey anti-mouse antibodies conjugated to Alexa Fluor®568 and donkey anti-goat antibodies conjugated to Alexa Fluor®568. α SMA was stained and visualized by incubating explants overnight with mouse monoclonal anti- α SMA conjugated to fluorescein isothiocyanate (FITC) (1:200; Sigma Aldrich Co. Oakville, ON, Canada). Explants were washed three times for 10 minutes per wash using PBS and mounted using Prolong Gold antifade reagent with DAPI (Invitrogen, Life Technologies). Fluorescence was detected using Leica DM6 fluorescence microscope at 40X. $n = 3$ experiments were

conducted for each assessed protein, where $n \geq 3$ explants were used per treatment for each experiment.

3.4 Western Blot Analysis

Rat LEC explants were collected and lysed in a protease inhibitor cocktail containing lysis buffer (50mM Tris-HCl, pH=8.0, 150mM NaCl and 1% Triton X-100) and a protease inhibitor (Roche Diagnostics, Germany). Protein concentration from each sample was estimated using the DC Protein Assay (Bio-Rad) in a microplate, and 20 μ g of protein per treatment group ($n \geq 10$ explants per treatment were collected for each experiment) was prepared and loaded into a pre-casted 10-well Mini-PROTEAN® TGX™ gel (Bio-Rad) to perform SDS-PAGE. Resolved bands were transferred to a nitrocellulose membrane (Pall Corporation). Ponceau was used to detect the presence of proteins, and the membrane was washed with tris-buffered saline (TBS) until the ponceau stain was reversed. The membrane was cut and blocked using Odyssey® blocking buffer (PBS) (LI-COR Biosciences) for 1 hour at room temperature. The blocked membrane was incubated with primary antibodies for cortactin (1:1000; Invitrogen) and GAPDH (1:1000; Abcam) overnight at 4°C. The blots were washed 3 times for 10 minutes per wash with 1% Tween-20 in TBS, and incubated with secondary antibodies, donkey anti-rabbit IRDye® 680 LT (1:10000; Mandel Scientific) or anti-mouse IRDye® 800 CW (1:10000; Mandel Scientific), at room temperature for 1 hour with gentle shaking. The membrane was visualized using the Odyssey near-infrared scanning system (LI-COR Biosciences). The experiment was conducted 3 times, and protein quantification was determined using Image J software. Average protein levels, standard deviation and p-values were calculated using Microsoft Excel.

CHAPTER FOUR

Results

4.1 Aim 1: Validate the MMP9-specific inhibitor, JNJ0966, for use in rat LEC explants.

JNJ0966, a novel MMP-9-specific allosteric inhibitor of activation was identified and tested for its potential to prevent TGF- β 2-induced EMT (Scannevin *et al.*, 2017). This inhibitor has no effect on the catalytic activities of other MMPs including MMP1, MMP2 and MMP14 (Scannevin *et al.*, 2017). Since the IC_{50} of JNJ0966 is 440nM, and 10 μ M was the maximum concentration used for MMP activity assays, initial experiments were conducted using pre-treatments of JNJ0966 at 1 μ M, 5 μ M and 10 μ M (Scannevin *et al.*, 2017). However, after being treated with TGF- β 2 for 48 hours, capsular wrinkling and the cell elongation were observed in all pre-treated groups. Therefore, increased concentrations, 10 μ M, 15 μ M and 20 μ M, were used to test the efficacy of JNJ0966 in preventing TGF- β 2-induced EMT (Figure 14). A 2-hour pre-treatment with 20 μ M of JNJ0966 was observed to be able to prevent the elongation of rat LEC explants that have then been exposed to 6ng/mL of TGF- β 2 (TG:JNJ) for 48 hours (Figure 14). Immunofluorescence analysis was also conducted to further confirm the efficacy of JNJ0966 in preventing TGF- β 2-induced EMT. Figure 15 shows elevated levels of α SMA in LECs treated with TGF- β 2 (TG) when compared to LECs treated with dimethyl sulfoxide (DMSO control), which was the solvent for JNJ0966. More importantly, LECs that were only treated with 20 μ M JNJ0966 (JNJ) and TG:JNJ LECs showed similar α SMA immunofluorescence staining as DMSO controls (Figure 15). To provide additional assurance that JNJ0966 prevents TGF- β 2-induced EMT, the presence of E-cadherin was also analyzed. As expected, E-cadherin was present and localized to cell margins in DMSO control, JNJ and TG:JNJ LECs, but E-cadherin was reduced and delocalized in TG LECs (Figure 15).

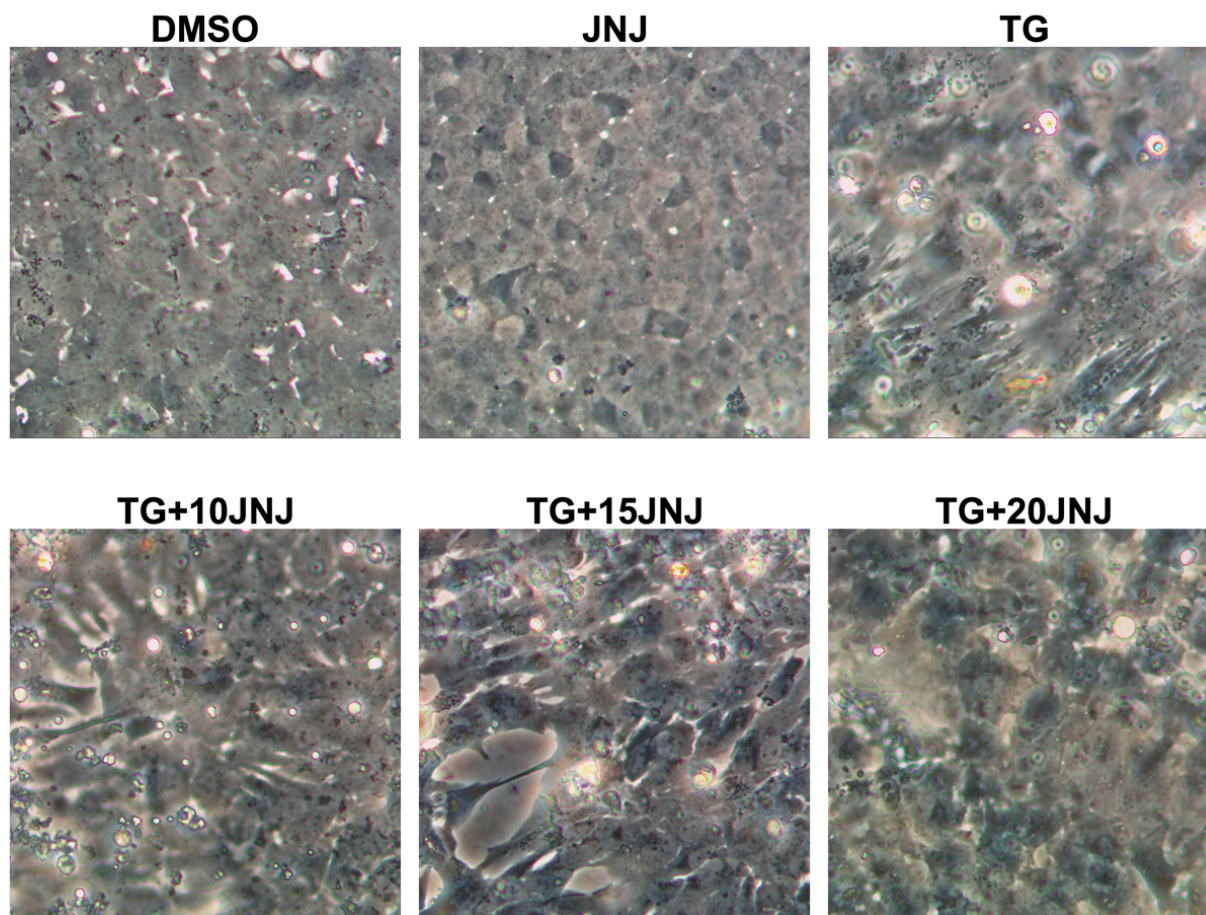


Figure 14. Images of LECs upon JNJ0966 treatment. Rat LEC explants were treated with <math><0.5\%</math> DMSO, 6ng/mL TGF- β 2 for 48 hours (TG), 20 μ M JNJ0966 (JNJ) for 48 hours, or pretreated with 10 μ M (TG+10JNJ), 15 μ M (TG+15JNJ) or 20 μ M JNJ0966 (TG+20JNJ) for 2 hours followed by 6ng/mL TGF- β 2 for 48 hours ($n = 3$ experiments, where $n \geq 3$ explants per treatment were used for each experiment). Photographs were acquired at 48 hours post-TGF- β 2 treatment with Leica DM IL LED microscope at 20X and the Moticam BTU camera.

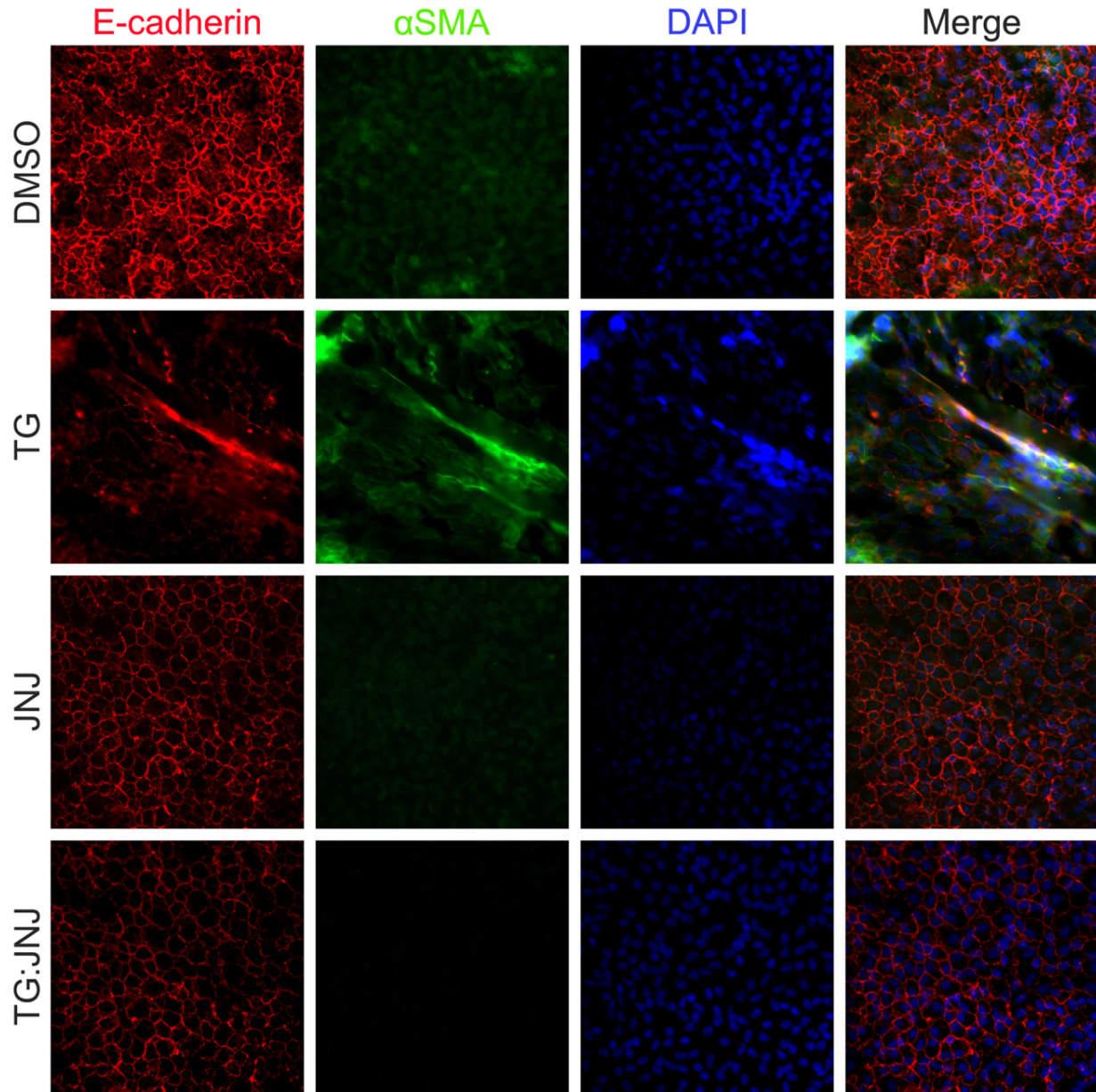


Figure 15. Expression and localization of E-cadherin and α SMA. Rat LEC explants were treated with <0.05% DMSO, 10 ng/mL TGF- β 2 for 48 hours (TG), 20 μ M JNJ0966 (JNJ) for 48 hours, or pretreated with 20 μ M JNJ0966 for 2 hours followed by 10ng/mL TGF- β 2 for 48 hours (TG:JNJ) ($n = 3$ experiments, where $n \geq 3$ explants per treatment were used for each experiment). Paraformaldehyde (PFA) fixed explants were stained for E-cadherin (red) and α SMA (green), and mounted with DAPI to visualize the nuclei. Images were acquired using Leica DM6 fluorescence microscope at 40X.

4.2 Aim 2. Identify MMP9-dependent signalling molecules in stress fibre formation of TGF- β -induced EMT in the lens.

Previous work from our laboratory revealed that actin polymerization was affected by the lack of MMP9 (Figure 11). Therefore, a cytoskeletal protein array was conducted to analyse the differential regulation of potentially affected proteins. Cortactin, focal adhesion kinase (FAK), lim-domain kinase-1 (LIMK1) and myosin light chain-2 (MLC2) were selected for validation based on fold changes of 1.5 between TGF- β 2 treated and untreated wildtype mouse LECs and their central roles in actin polymerization and stabilization (Figure 10). A 3.11-fold increase in cortactin, known to be critical for F-actin polymerization and branching (Bamburg and Bernstein, 2010), levels was observed between TG (7.11 ± 0.04) and control (2.29 ± 0.0005) LECs (Figures 13 and 16A; **** $p < 0.0001$). However, no marked difference in cortactin levels was observed in MMP9KO-TG LECs (3.63 ± 0.002) when compared to untreated un-MMP9KO LECs (2.90 ± 0.07) (Figures 13 and 16A; **** $p < 0.0001$). Another important protein that showed a notable difference in expression was FAK, a major component of focal adhesion complexes that has been shown to play critical roles in actin cytoskeletal remodeling, stress fibre formation and cell migration (Parsons, 2003) (Mitra *et al.*, 2005) (Schwack and Dhani, 2011). The expression of FAK was upregulated in TG LECs (29.1 ± 0.2) by 2.34-fold in comparison to control LECs (12.41 ± 0.05) (Figures 13 and 16B; **** $p < 0.0001$). The MMP9KO-TG LECs (20.7 ± 0.3) failed to show a notable upregulation of FAK when compared to un-MMP9KO LECs (20.11 ± 0.02) (Figures 13 and 16B; * $p < 0.05$). In addition, we observed a 1.27-fold increase in phosphorylated, and therefore activated, FAK (pFAK) in TG LECs when compared to control LECs, but no marked upregulation of pFAK was observed between MMP9KO-TG and un-MMP9KO LECs (Figure 13). Another protein that was differentially regulated was LIMK1,

which is a major regulator of actin dynamics that functions by phosphorylating and inhibiting the key actin-depolymerizing protein, cofilin (Prunier *et al.*, 2017). LIMK1 is also involved in the modulation of microtubule dynamics by promoting microtubule depolymerization (Prunier *et al.*, 2017). The expression of LIMK1 was observed to be upregulated by 2.85-fold in TG LECs (3.75 ± 0.03) when compared to control LECs (1.31 ± 0.001) (Figures 13 and 16C; **** $p < 0.0001$), but no marked upregulation was observed between MMP9KO-TG (3.76 ± 0.04) and un-MMP9KO (3.49 ± 0.01) LECs (Figures 13 and 16C; *** $p < 0.001$). Furthermore, the phosphorylation, and therefore activation, of LIMK1 (pLIMK1) was 1.26-fold higher in TG LECs when compared to control LECs, but this upregulation was also not observed between MMP9KO-TG and un-MMP9KO LECs (Figure 13). MLC2 is crucial for myosin-actin cross-bridge cycling and contractility (Sheikh *et al.*, 2015), and therefore the upregulation and activation of MLC2 indicate increased contractility of LECs. We observed a 1.74-fold increase in MLC2 levels between TG (2.95 ± 0.02) and control LECs (1.69 ± 0.004) (Figures 13 and 16D; **** $p < 0.0001$), but this upregulation was not observed between MMP9KO-TG (1.89 ± 0.03) and un-MMP9KO LECs (1.79 ± 0.002) (Figures 13 and 16D; ** $p < 0.01$). We also observed a 1.54-fold increase in phosphorylated, and therefore activated, MLC2 (pMLC2) between TG and control LECs, but no marked difference in pMLC2 was observed between MMP9KO-TG and un-MMP9KO LECs (Figure 13).

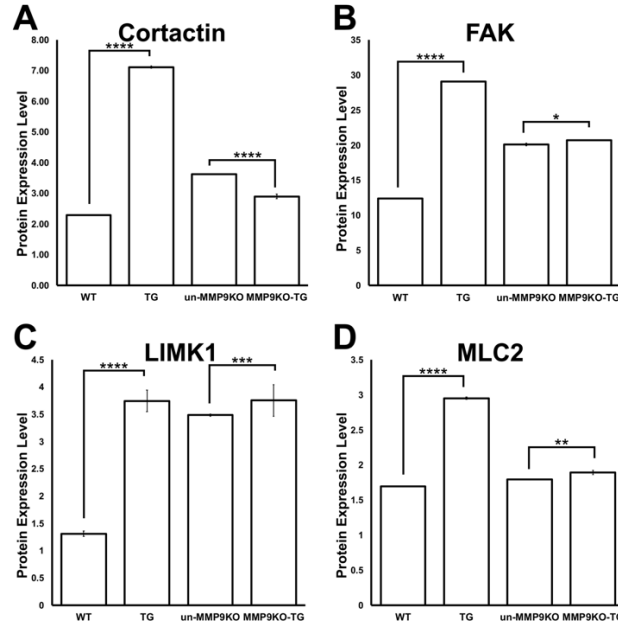


Figure 16. Protein expression levels of selected proteins. Graphs show the average signals for protein expression that were normalized to the median signal of the endogenous control, GAPDH. Cytoskeletal protein array analysis was conducted using LEC explants from wildtype mice that were left untreated (control) or treated with 500pg/mL TGF- β for 72 hours (TG), and MMP9KO mice that were left untreated (un-MMP9KO) or with treated with 500 pg/mL TGF- β for 72 hours (MMP9KO-TG). Cortactin (A), focal adhesion kinase (FAK) (B), lim-domain kinase-1 (LIMK1) (C) and myosin light chain-2 (MLC2) (D) were selected for validation. Error bars indicate the standard deviation of the average protein expression level. ($n = 3$ experiments, where 10 μ g of protein per treatment was used for each experiment; * $p < 0.05$; ** $p < 0.01$; ***; $p < 0.001$; **** $p < 0.0001$). Experiment performed by Dr. Aftab Taiyab (unpublished).

With the above protein array data, and the confirmation that the treatment with JNJ0966 prevented TGF- β 2-induced EMT in rat LECs, the expression and localization of the proteins of interest were validated and assessed using immunohistochemistry and western blot analyses. The first protein that was assessed was cortactin, and western blot analysis showed a significant upregulation of cortactin between TG and DMSO control rat LECs ($n = 3$ experiments; * $p < 0.05$) (Figures 17A and B). The protein levels were not significant between TG:JNJ and JNJ LECs ($n = 3$ experiments; $p > 0.5$) (Figure 17B). In addition, cortactin was notably upregulated and delocalized in TG rat LECs in comparison to the DMSO control (Figure 17C).

Immunofluorescence staining for cortactin in JNJ and TG:JNJ LECs resembled that of the DMSO controls (Figure 17C).

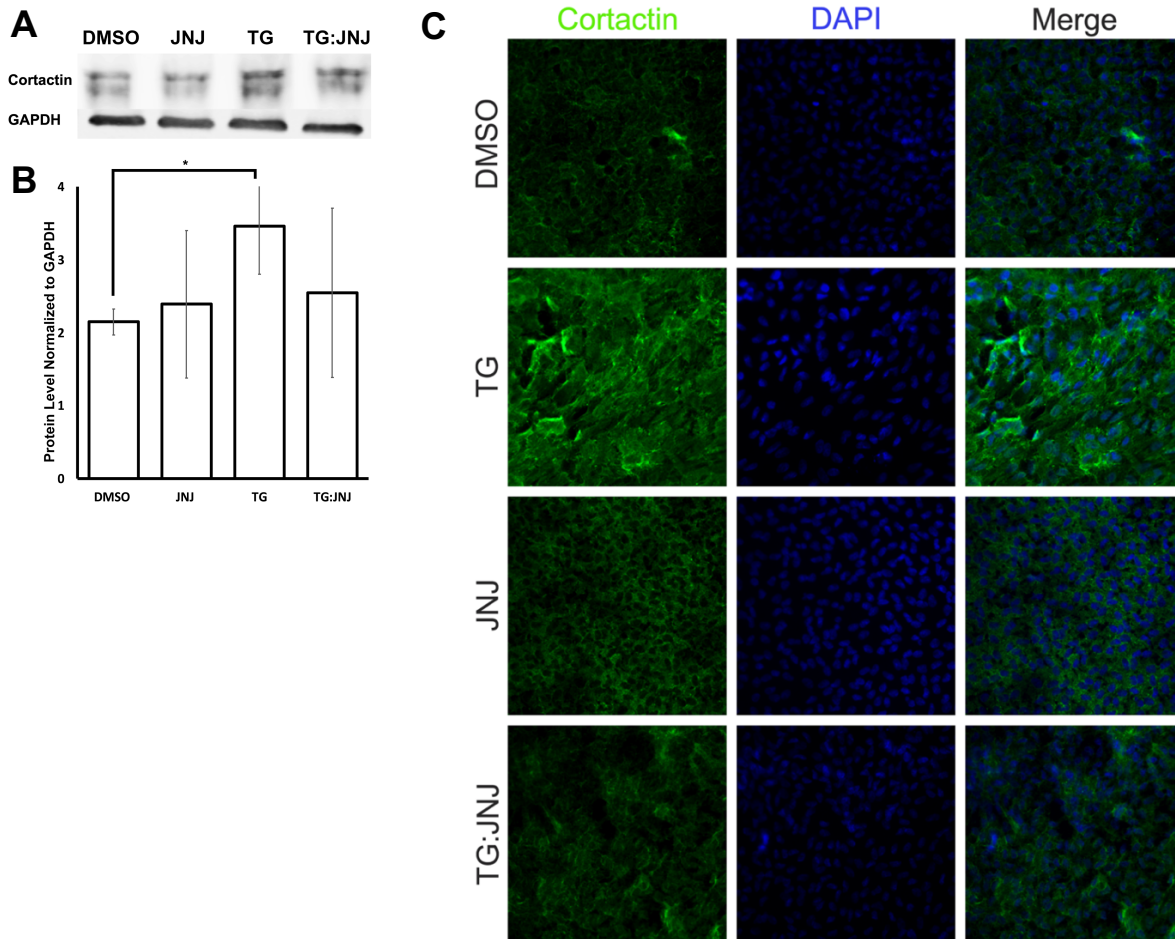


Figure 17. Expression and localization of cortactin. Rat LEC explants were treated with DMSO, 6ng/mL TGF- β 2 for 48 hours (TG), 20 μ M JNJ0966 (JNJ) for 48 hours, or pretreated with 20 μ M JNJ0966 for 2 hours followed by 6ng/mL TGF- β 2 for 48 hours (TG:JNJ) **A**: Representative western blots of cortactin and the endogenous control, GAPDH. Rat LEC explants were collected and lysed in a protease inhibitor cocktail, and 20 μ g of protein per treatment was used loaded into a polyacrylamide gel to perform SDS-PAGE. A wet transfer to a nitrocellulose gel was performed, and ponceau was used to detect protein presence. The membrane was blocked and probed for cortactin and GAPDH and visualized using Odyssey near-infrared scanning system and analyzed using Image J software ($n = 3$ experiments). **B**: graph shows the average protein level after being normalized to the endogenous control, GAPDH. Error bars indicate \pm standard deviation of the average protein levels from the western blots ($n = 3$ experiments, where 20 μ g of protein per treatment was used per experiment; * $p < 0.05$) **C**: Image shows immunofluorescence staining for cortactin. Paraformaldehyde (PFA) fixed explants were stained for cortactin (green) and mounted with DAPI to visualize the nuclei. Images were acquired using Leica DM6 fluorescence microscope at 40X ($n = 3$ experiments where $n \geq 3$ explants per treatment were used for each experiment).

Immunofluorescence analyses also revealed that FAK and α SMA were upregulated in TG LECs in comparison to DMSO control LECs (Figure 18). However, FAK expression was also upregulated in TG:JNJ LECs in comparison to JNJ LECs, but no noticeable α SMA expression was observed in either TG:JNJ or JNJ LECs (Figure 18). Since TGF- β upregulated overall FAK in MMP9-inhibited LECs, the autophosphorylation of FAK at Tyr397 (pFAK), which indicates the protein's activation (Grigera *et al.*, 2005), was further analyzed. Immunofluorescence analyses indicated that pFAK and α SMA levels were elevated in TG LECs in comparison to DMSO control, JNJ and TG:JNJ LECs (Figure 19).

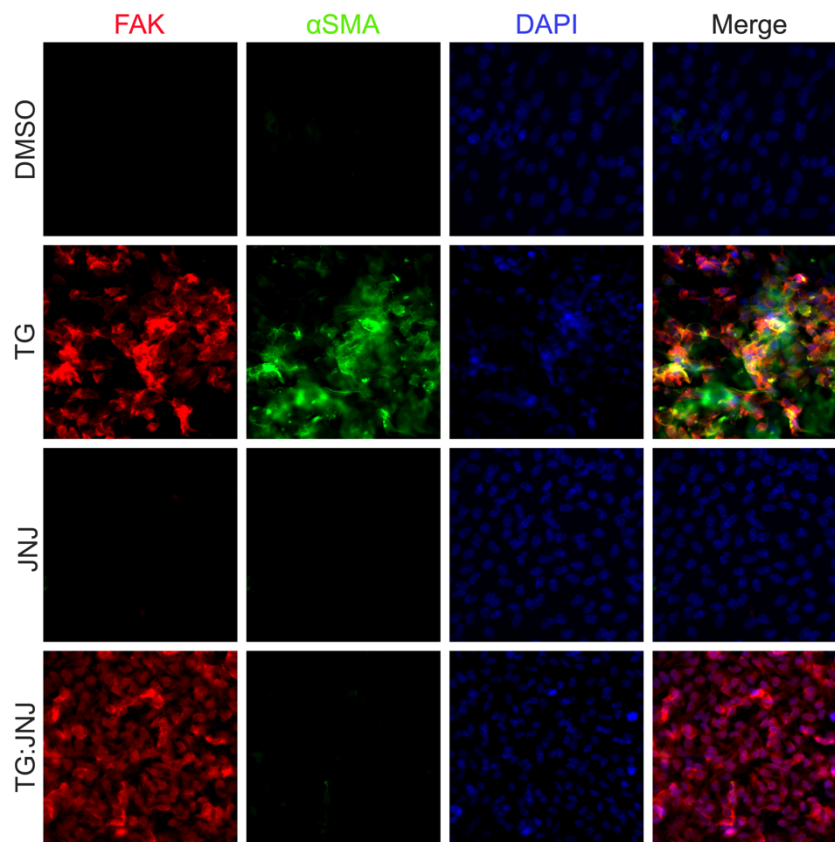


Figure 18. Expression and localization of focal adhesion kinase (FAK). Rat LEC explants were treated with DMSO, 6ng/mL TGF- β 2 for 48 hours (TG), 20 μ M JNJ0966 (JNJ) for 48 hours, or pretreated with 20 μ M JNJ0966 for 2 hours followed by 6ng/mL TGF- β 2 for 48 hours (TG:JNJ) ($n = 3$ experiments, where $n \geq 3$ explants per treatment were used for each experiment). Paraformaldehyde (PFA) fixed explants were stained for FAK (red) and α SMA (green) and mounted with DAPI to visualize the nuclei. Images were acquired using Leica DM6 fluorescence microscope at 40X.

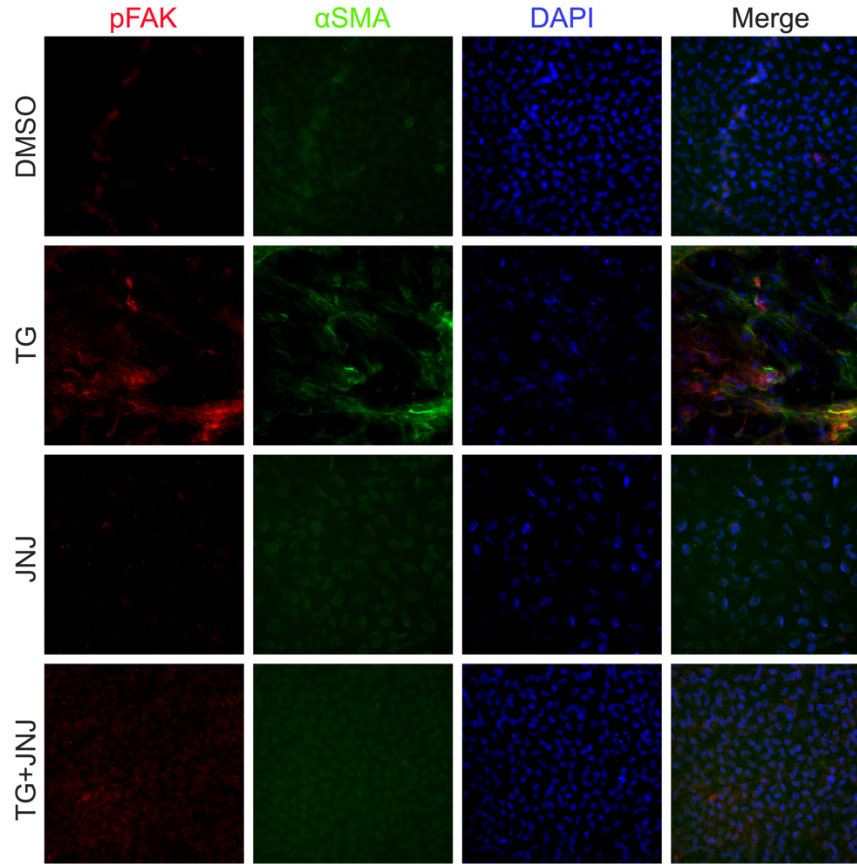


Figure 19. Expression and localization of phosphorylated focal adhesion kinase at Tyr397 (pFAK). Rat LEC explants were treated with DMSO, with 6ng/mL TGF- β 2 for 48 hours (TG), with 20 μ M JNJ0966 (JNJ) for 48 hours, or pretreated with 20 μ M JNJ0966 for 2 hours followed by 6ng/mL TGF- β 2 for 48 hours (TG:JNJ) ($n = 3$ experiments where $n \geq 3$ explants per treatment were used for each experiment). Paraformaldehyde (PFA) fixed explants were stained for pFAK (red) and α SMA (green) and mounted with DAPI to visualize the nuclei. Images were acquired using Leica DM6 fluorescence microscope at 40X.

The next protein that was analyzed was LIMK1, which was upregulated in TG, JNJ and TG:JNJ LECs when compared to DMSO control LECs (Figure 20). However, the localization of LIMK1 was nuclear in JNJ and TG:JNJ LECs, and α SMA was not observed, when compared to more diffuse cytoplasmic and nuclear localizations of LIMK1, and α SMA expression, in TG LECs (Figure 20). Since no noticeable difference in LIMK1 expression was detected between JNJ and TG:JNJ LECs, additional experiments were performed to analyze the phosphorylation of LIMK1 at Thr508 (pLIMK1) that indicates the protein's activation (Ohashi *et al.*, 2000).

Immunofluorescence staining from figure 21 shows upregulations of pLIMK1 in TG and TG:JNJ LECs when compared to DMSO control and JNJ LECs respectively, but α SMA was observed to be upregulated in TG LECs only. Furthermore, the localization of pLIMK1 was cytoplasmic and nuclear in TG LECs, but pLIMK1 was limited to the nucleus in JNJ and TG:JNJ LECs (Figure 21).

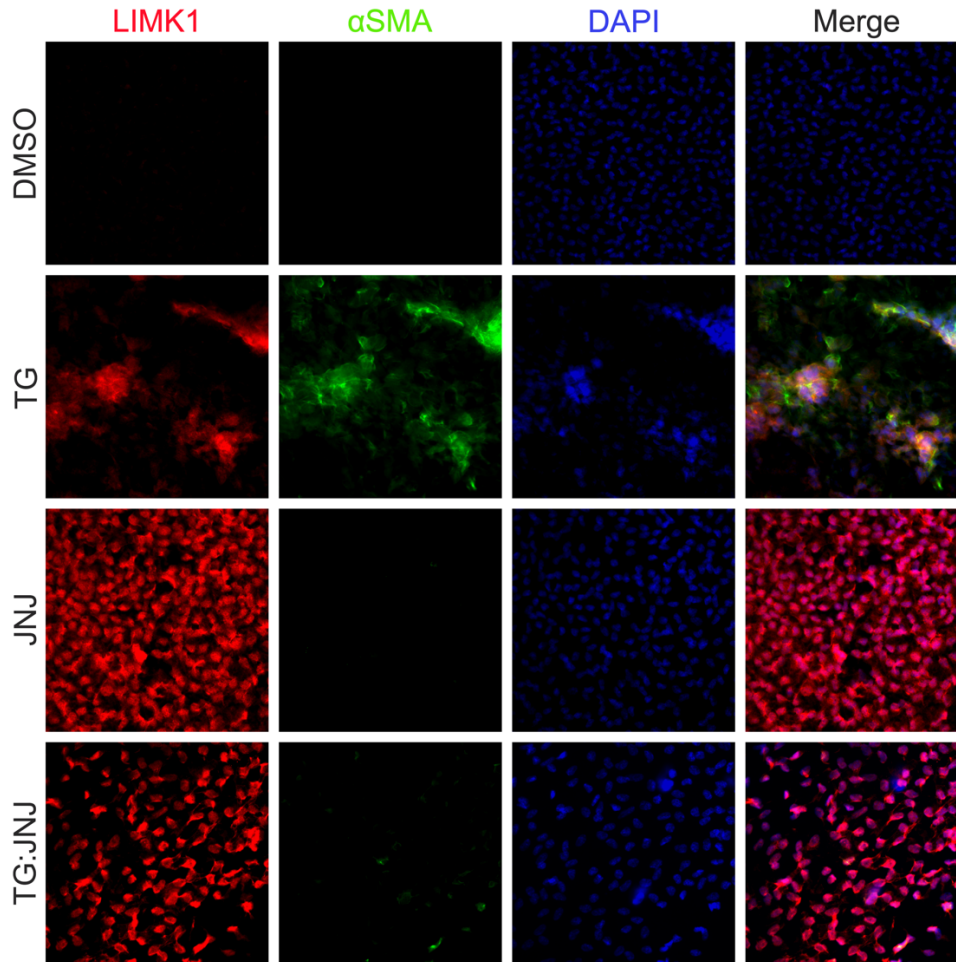


Figure 20. Expression and localization of lim-domain kinase-1 (LIMK1). Rat LEC explants were treated with <5% DMSO, 6ng/mL TGF- β 2 for 48 hours (TG), 20 μ M JNJ0966 (JNJ) for 48 hours, or pretreated with 20 μ M JNJ0966 for 2 hours followed by 6ng/mL TGF- β 2 for 48 hours (TG:JNJ) ($n = 3$ experiments, where $n \geq 3$ explants per treatment were used for each experiment). Paraformaldehyde (PFA) fixed explants were stained for LIMK1 (red) and α SMA (green), and mounted with DAPI to visualize the nuclei. Images were acquired using Leica DM6 fluorescence microscope at 40X.

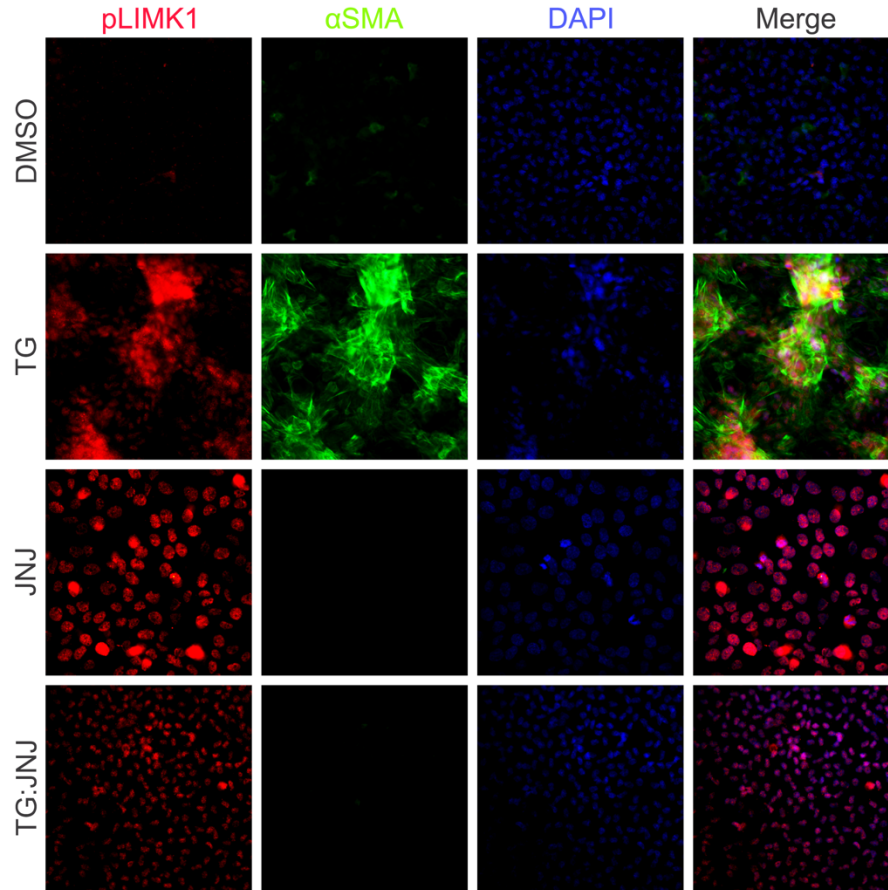


Figure 21. Expression and localization of phosphorylated lim-domain kinase-1 at Thr508 (pLIMK1). Rat LEC explants were treated with <5% DMSO, 6ng/mL TGF- β 2 for 48 hours (TG), 20 μ M JNJ0966 (JNJ) for 48 hours, or pretreated with 20 μ M JNJ0966 for 2 hours followed by 6ng/mL TGF- β 2 for 48 hours (TG:JNJ) ($n = 3$ experiments, where $n \geq 3$ explants per treatment were used for each experiment). Paraformaldehyde (PFA) fixed explants were stained for pLIMK1 (red) and α SMA (green), and mounted with DAPI to visualize the nuclei. Images were acquired using Leica DM6 fluorescence microscope at 40X.

It was noted from the protein array that the median protein level of phosphorylated MLC2 was greater than that of overall MLC2 in un-MMP9KO mouse LECs (2.95 versus 1.79 respectively) and MMP9KO-TG mouse LECs (2.14 versus 1.89 respectively). Therefore, the phosphorylated form of MLC2 (pMLC2) was selected for further validation.

Immunofluorescence staining for pMLC2 at Ser18 showed an upregulation of pMLC2 and α SMA in TG LECs when compared to DMSO control, JNJ and TG:JNJ LECs (Figure 22).

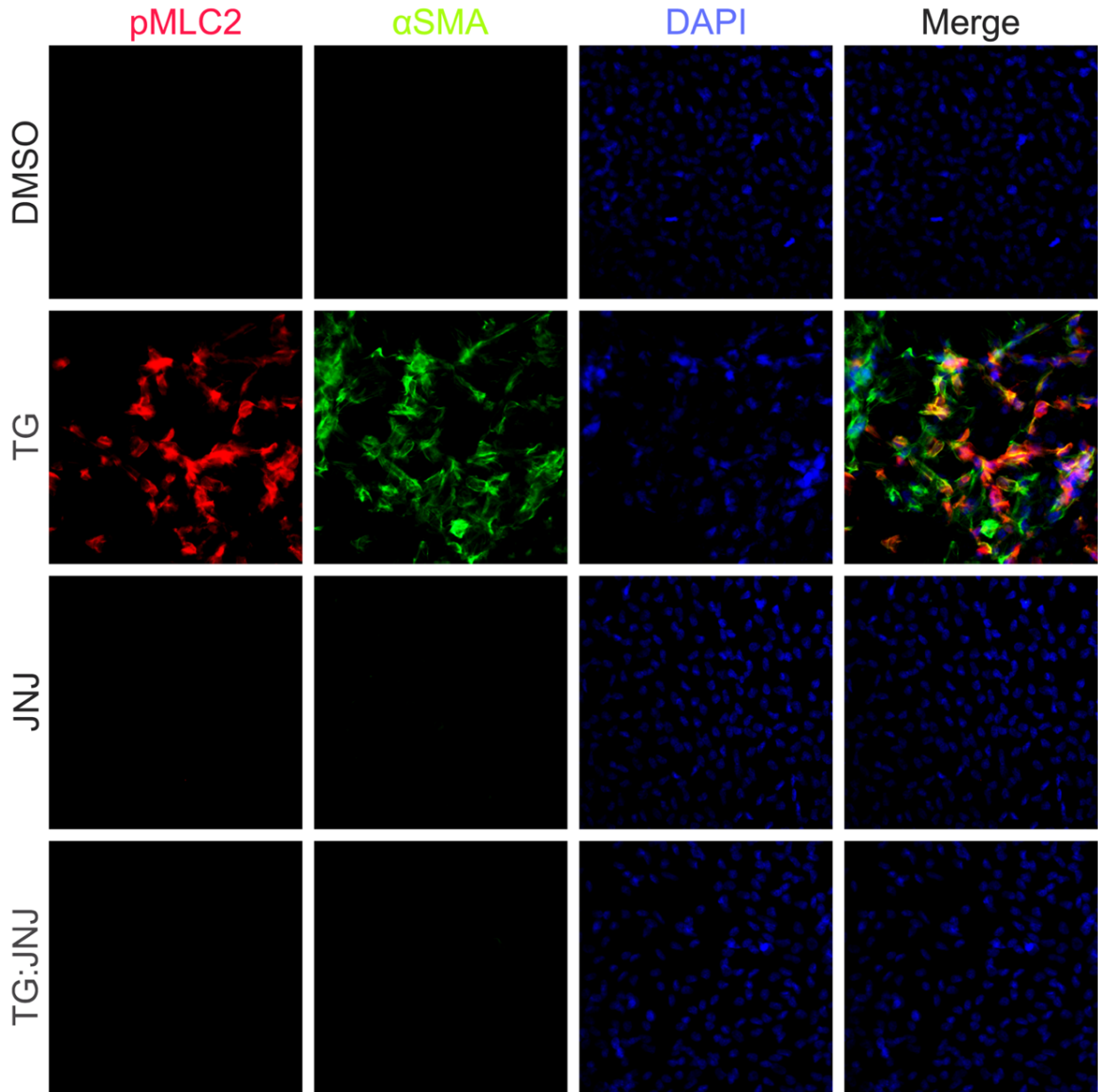


Figure 22. Localization of phosphorylated myosin light chain-2 at Ser18 (pMLC2). Rat LEC explants were treated with <5% DMSO, with 6ng/mL TGF- β 2 for 48 hours (TG), with 20 μ M JNJ0966 (JNJ) for 48 hours, or pretreated with 20 μ M JNJ0966 for 2 hours followed by 6ng/mL TGF- β 2 for 48 hours (TG:JNJ) ($n = 3$ experiments, where $n \geq 3$ explants per treatment were used for each experiment). Paraformaldehyde (PFA) fixed explants were stained for pMLC2 (red) and α SMA (green) and mounted with DAPI to visualize the nuclei. Images were acquired using Leica DM6 fluorescence microscope at 40X.

4.3 Aim 3: Reveal MMP9-dependent pathways that result in cytoskeletal modification during TGF- β -induced EMT of the lens.

Since the actin polymerization machinery appeared to be inactive in MMP9-inhibited explants, we proposed that the Rho/ROCK pathway and the downstream dissociation of G-actin from MRTF-A to provide actin monomers for polymerization were affected (Korol, 2017). The lack of dissociation of G-actin from MRTF-A would result in reduced MRTF-A translocation to the nucleus and therefore decreased transcription of key EMT-associated genes, including *MMP9* (Gupta *et al.*, 2013) (Korol, 2017). Hence, immunofluorescence staining for MRTF-A was performed by using rat LECs and JNJ0966. Figure 23 shows nuclear localization of MRTF-A in TG rat LECs as the red MRTF-A stain co-localized almost perfectly with DAPI. Cytoplasmic localization of MRTF-A was observed in DMSO control and JNJ LECs (Figure 23). However, some MRTF-A seemed to be co-localized with DAPI in TG:JNJ LECs, which indicates some presence of nuclear MRTF-A, but its presence was still mostly in the cytoplasm (Figure 23).

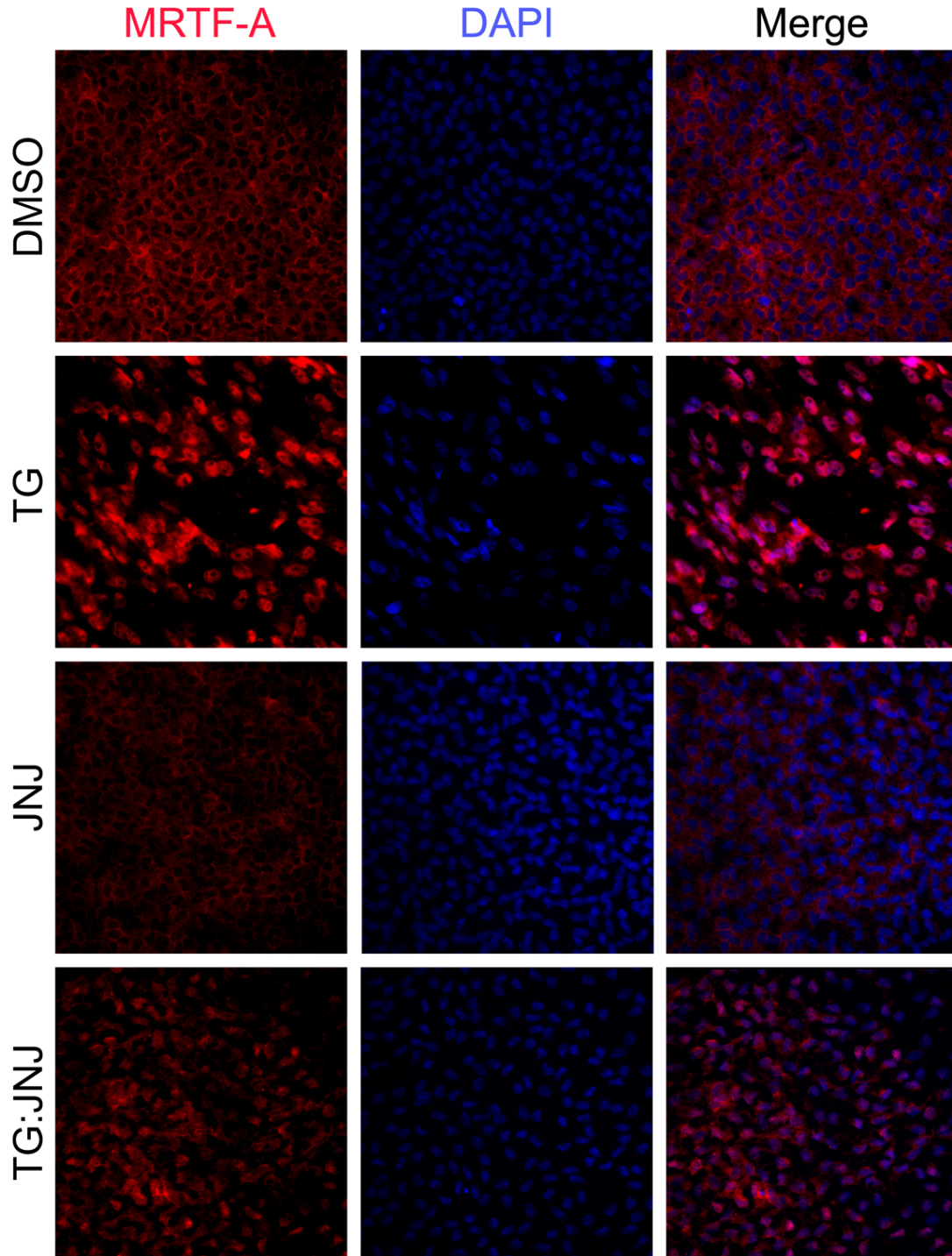


Figure 23. Expression and localization of myocardin-related transcription factor-A (MRTF-A). Rat LEC explants were treated with <5% DMSO, 6ng/mL TGF- β 2 for 48 hours (TG), 20 μ M JNJ0966 (JNJ) for 48 hours, or pretreated with 20 μ M JNJ0966 for 2 hours followed by 6ng/mL TGF- β 2 for 48 hours (TG:JNJ) ($n = 3$ experiments, where $n \geq 3$ explants per treatment were used for each experiment). Paraformaldehyde (PFA) fixed explants were stained for MRTF-A (red) and mounted with DAPI to visualize the nuclei. Images were acquired using Leica DM6 fluorescence microscope at 40X.

CHAPTER FIVE

Discussion

5.1 Discussion

Understanding the mechanisms by which TGF- β induces EMT and fibrosis is crucial for the development of therapeutics for preventing this irreversible condition in organ systems including the lens, lungs and kidneys (Guarino *et al.*, 2009). One of the major modifications to cells and organs during TGF- β induced fibrosis is the aberrant deposition of ECM components, and intracellular cytoskeletal remodelling (Kalluri and Weinburg, 2009). MMP9, which is one of the two gelatinases, is upregulated and can degrade healthy collagen IV in the ECM. These healthy ECM components are subsequently replaced with EMT-associated ECM components such as fibronectin and collagens I and III (Eldred *et al.*, 2014). KO studies from our laboratory have revealed the requirement of MMP9, but not the other gelatinase MMP2, in TGF- β -induced EMT in the mouse lenses (Korol *et al.*, 2014). More interestingly, the cytoskeleton was modified in MMP9KO mouse LECs, and such modifications were not observed in MMP2KO mouse LECs (Korol *et al.*, 2014). Therefore, using the LEC explant model, our laboratory aimed to understand the cytoskeletal components that were modified due to the MMP9 deficiency and the roles these proteins play in TGF- β -induced EMT. Immunofluorescence staining showed that there was a lack of F-actin and α SMA stress fibre formation in MMP9KO mouse LECs that were treated with TGF- β 2 (Figure 11) (Korol *et al.*, 2014). To further confirm these observations, a NanoString analysis was performed which showed no notable differences in the mRNA expressions of α SMA (*ACTA2*) and β -actin (*ACTB*) between TGF β^{tg} and TG:JNJ mouse lenses (Figures 12B and C). Since actin mRNA expression was not observed to be affected, but F-actin and α SMA protein expression were absent in MMP9KO mouse LECs when stimulated with TGF- β 2, we surmised that the actin polymerization machinery was differentially regulated at the protein level as a result of the MMP9 deficiency.

As outlined above, previous investigations into the role of MMP9 in regulating TGF- β -induced EMT were conducted using mouse LECs. The discovery of the novel MMP9-specific, JNJ0966, led to the potential of completing experiments using our *ex vivo* LEC models, which can recapitulate the *in vivo* situation of the cells (West-Mays *et al.*, 2010). The inhibitor would allow for the use of rat LEC explants which could provide more protein per explant than mouse explants. The use of rat LEC explants would also allow for the experiments to be completed more efficiently as transgenic KO animals would not need to be housed and bred. Unlike previously available inhibitors that targeted the active site, JNJ0966 targeted MMP9 allosterically by hindering its activation (Scannevin *et al.*, 2017). In addition, Scannevin *et al.* have shown that 10 μ M of JNJ0966 significantly reduced the activation of MMP9 by trypsin (***) $p < 0.001$) in comparison to DMSO controls, but the activation of MMP2 by MMP14 was not significantly different from DMSO controls. Crystallization experiments were conducted by Scannevin *et al.* (2017) and suggested that JNJ0966 interacts with specific amino acid residues in the activation domain (“binding pocket”) of pro-MMP9. Therefore, amino acid point mutations for residues in this binding pocket were generated in pro-MMP9, and a gelatinase activation assay was conducted using catalytic MMP3 as the activator of MMP9 (Scannevin *et al.*, 2017). It was revealed that single alanine substitutions at Phe-110 and Tyr179 reduced the efficacy of JNJ0966 (Scannevin *et al.*, 2017). Triple alanine substitutions at sites Val-101, Phe-110 and Tyr179 rendered JNJ0966 completely ineffective as MMP9 was able to be fully activated by MMP3 (Scannevin *et al.*, 2017). Although 10 μ M seemed to prevent the activation of MMP9 by trypsin or MMP3 in the initial study (Scannevin *et al.*, 2017), 20 μ M of JNJ0966 was needed to prevent TGF- β 2-induced EMT in rat LECs (Figure 15). Pre-treatments with 20 μ M of JNJ0966 prevented the elongation of cells, expression of α SMA and delocalization of E-cadherin in rat

LECs that were subsequently treated with 6-10 ng/mL of TGF- β 2 (TG:JNJ) (Figures 14 and 15). With the above results, JNJ0966 was deemed effective at preventing TGF- β 2-induced EMT because it prevented the development of mesenchymal characteristics, and epithelial characteristics of cuboidal rat LECs were maintained. The specificity of JNJ0966 for MMP9 at the elevated concentration of 20 μ M remains unclear. However, as mentioned previously, the other related gelatinase, MMP2 was previously shown by our research group to not be essential for TGF- β 2-induced EMT. In addition, cytoskeletal modifications that were observed in TGF- β 2 treated MMP9KO LEC explants were not observed in TGF- β 2 treated MMP2KO mouse LECs. Therefore, any cross-inhibition of MMP2 that may have occurred due to the increased concentration of JNJ0966 that was used should not affect the results of this experiment. Nevertheless, western blot analysis or zymography should be conducted in the future for different MMPs using the media from rat LEC explants that were treated with 20 μ M of JNJ0966 and TGF- β 2 in order to confirm the specificity of the inhibitor for MMP9 in rat LEC explants at this increased concentration.

In order to understand which components of the actin polymerization pathways were differentially regulated when MMP9 is absent, a cytoskeletal protein array was conducted using TGF- β 2 treated and untreated wildtype and MMP9KO mouse LECs. Of the numerous proteins that are differentially regulated by the MMP9 deficiency, cortactin, FAK, LIMK1 and MLC2 were selected for validation via western blot and immunofluorescence analyses. The first protein that was assessed was cortactin, as the array showed a notable upregulation of cortactin between TGF- β 2 treated wildtype (TG) and untreated wildtype (control) mouse LECs, but this upregulation was not observed between TGF- β 2 treated MMP9KO (MMP9KO-TG) and untreated MMP9KO (un-MMP9KO) mouse LECs (Figures 13 and 16A). This protein array

result was confirmed as only the upregulation of cortactin between TGF- β 2 treated (TG) and <0.5% treated DMSO (DMSO control) was notable and significant (Figure 17B; * $p < 0.05$) in the western blot. Immunofluorescence staining for cortactin further validated the protein array results as cortactin was only upregulated in TG rat LECs, and JNJ and TG:JNJ rat LECs showed similar staining to DMSO controls (Figure 17C). Cortactin is known to bind and activate the Arp2/3 complex, which has crucial roles in actin polymerization by promoting actin nucleation and branching (Daly, 2004) (Bamburg and Bernstein, 2010) (Weed *et al.*, 2000). Therefore, the lack of cortactin upregulation in TGF- β 2 treated and MMP9 deficient LECs could suggest that the actin nucleation and branching steps during F-actin formation were hindered, and thus F-actin formation could not occur in the MMP9KO mouse LECs (Figure 11). In addition, cortactin binds to newly added actin subunits with ATP or ADP-Pi (Bamburg and Bernstein, 2010), and is therefore also involved in the maintenance of F-actin filaments. The lack of cortactin upregulation in MMP9 deficient models seemed to suggest that not only was the formation of actin affected, but the maintenance of F-actin filaments may also have been reduced. Furthermore, the localization of cortactin in cortical areas of the cell, especially if co-localized with actin, is associated with cell migration (Daly, 2004), and cell migration is a characteristic of LECs that have transformed into myofibroblasts during PCO (Wormstone, 2002). During analysis via immunohistochemistry, we observed perinuclear localization of cortactin in TG:JNJ rat LECs that was similar to JNJ and DMSO controls (Figure 17C). This result suggests that only TG LECs, which showed cortical localization and striated immunofluorescence staining of cortactin had the potential to migrate (Figure 17C). In addition, the cell shape of TG LECs also appeared to be elongated, as defined by the striations of the cortactin staining, and this elongated

cell shape acts as further evidence that TGF- β 2-induced EMT wasn't observed in TG:JNJ LECs (Figure 17C).

While cortactin binds to newly added actin subunits, cofilin, an actin-depolymerizing protein binds to older subunits with ADP, and thus, promotes the degradation of F-actin polymers (Bamburg and Bernstein, 2010). LIMK1 is an important regulator of cofilin activity by phosphorylating and inhibiting cofilin at Ser3 (Prunier *et al.*, 2017). Therefore, the upregulation of LIMK1 could be responsible for F-actin maintenance during TGF- β -induced EMT through its inhibition of cofilin. More interestingly, although the protein array showed an upregulation of LIMK1 between TG and control mouse LECs and no marked upregulation between un-MMP9KO and MMP9KO-TG mouse LECs, an upregulation of LIMK1 was observed between un-MMP9KO and control mouse LECs. (Figures 13 and 16C). Upon validation via immunofluorescence staining, we observed a similar upregulation pattern where LIMK1 was upregulated between TG rat LECs when compared to DMSO control LECs, and the protein was not upregulated between JNJ and TG:JNJ rat LECs (Figure 20). However, similar to the protein array, LIMK1 was also upregulated in JNJ and TG:JNJ rat LECs in comparison to DMSO control rat LECs (Figure 20). More interestingly, the localization of LIMK1 was nuclear in JNJ and TG:JNJ rat LECs in comparison to cytoplasmic and nuclear localizations of LIMK1 in TG rat LECs (Figure 20). Investigations from other laboratories have shown that LIMK1 shuttles between the nucleus and cytoplasm, and that the differential ratios of nuclear and cytoplasmic LIMK1 could implicate cancer progression (Yang and Mizumo, 1999) (McConnell *et al.*, 2011). Further studies should be carried out via immunohistochemistry with MMP9KO mice to see if a similar staining pattern to figure 20 of this study is observed. If so, further analysis can be carried out to determine the nuclear and cytoplasmic ratios of LIMK1 in TGF- β 2 treated wildtype and

MMP9KO LECs. This will help determine the nuclear/cytoplasmic ratio at which the lack of MMP9 prevented TGF- β 2-induced EMT. The observation that the LIMK1 was upregulated in un-MMP9KO and MMP9KO-TG mouse LECs as well as in JNJ and TG:JNJ rat LECs, may offer indirect support that JNJ0966 is MMP9-specific.

Another protein that was observed to be differentially regulated in MMP9-deficient mouse LECs from the protein array was FAK (Figures 13 and 16B). FAK was upregulated in TG when compared to control mouse LECs, but no notable upregulation of FAK was observed between un-MMP9KO and TG-MMP9KO LECs (Figures 13 and 16B). However, an upregulation in FAK was observed in TG:JNJ rat LECs when compared to JNJ LECs, though the EMT marker, α SMA was not observed in either of the JNJ-treated LECs (Figure 18). The immunofluorescence staining also showed nuclear localization of FAK in TG:JNJ LECs, whereas it was localized to the cytoplasm in TG rat LECs (Figure 18). Some investigations have demonstrated the potential for FAK to be a co-transcriptional regulator during cancer progression, which differs from the traditional understanding of its roles in focal adhesions (Lim, 2013). However, there has yet to be investigations that observed nuclear localization of FAK in LECs and other EMT-mediated fibrosis models, and further research is needed to understand this. Interestingly, although FAK was upregulated in TG:JNJ LECs, its activation at the autophosphorylation site, Tyr397, was not (Figure 19) (Grigera *et al.*, 2005). FAK, a major component of focal adhesion complexes, and it has been shown to be upregulated and activated by integrin clustering after the cell experiences some form of mechanical trauma, and tremendous mechanical trauma is experienced by LECs during PCO surgery (Parsons, 2000) (Lee and Nelson, 2012). Activated FAK in focal adhesion complexes (FACs) plays critical roles in activating other FAC components including Src (Parsons, 2000). FAK mediates several

intracellular signalling pathways of integrin-mediated mechanotransduction that are responsible for cytoskeletal remodelling to increase cell contractility and migration (Parsons, 2000) (Lee and Nelson, 2012). FAK-activated Src could in turn phosphorylate FAK to reveal binding sites for proteins with SH3 domains (Mitra *et al.*, 2005). GAPs and GEFs contain these SH3 domains, and their binding to FAK result in their activation (Mitra *et al.*, 2005). GAPs and GEFs activates RhoA, Rac and CDC42 to mediate stress fibre, lamellipodia and filopodia formations respectively (Mitra *et al.*, 2005) (Schwock and Dhani, 2011). The lack of activated FAK in TG:JNJ cells could mean that these downstream pathways may not be activated, and therefore and the formation of stress fibres and lamellipodia, which is associated with cell migration may be affected (Mitra *et al.*, 2005). FAK activation also increases cell contractility, which is needed for cell migration, via two pathways that ultimately result in the phosphorylation of MLC (Sheikh *et al.*, 2015) (Lee and Nelson, 2012). The first pathway is through the Rho/ROCK by directly phosphorylating MLC, and the second is by activating the Ras/Raf/MEK/ERK pathway to indirectly activate MLC via MLCK (Parsons, 2003) (Lee and Nelson, 2012). MLC2 was only observed to be phosphorylated, and co-localized with α SMA, in TG rat LECs (Figure 22), and therefore both of the aforementioned pathways of MLC activation might be inactive in the absence of MMP9. Since FAK activation is stimulated by integrin clustering, the lack of MMP9 might prevent mechanical-stress induced integrin clustering, by not digesting healthy components of the ECM, and the rest of the mechanotransduction cascade involving FAK and MLC activation.

Our laboratory has shown that the lack of MMP9 in MMP9KO mouse LECs that were treated with TGF- β 2, prevented the dissociation of E-cadherin- β -catenin complexes, which prevented β -catenin from translocating to the nucleus where it can upregulate EMT-associated

genes (Korol, 2017). MRTF-A is another transcription factor that implicates TGF- β 2-induced fibrosis, and this protein is downstream of the Rho/ROCK pathway (Small *et al.*, 2010) (Kobayashi *et al.*, 2019) (Shiwen *et al.*, 2015). Our laboratory and others have shown that endogenous MRTF-A is localized to the cytoplasm and associated with monomeric G-actin (Gupta *et al.*, 2013), (Small *et al.*, 2010) (Kobayashi *et al.*, 2019) (Shiwen *et al.*, 2015). However, upon TGF- β stimulation, the upregulation of the Rho/ROCK pathway prompts for a greater supply of G-actin for F-actin and α SMA stress fibre formation, and thus, G-actin dissociates from MRTF-A (Small *et al.*, 2010) (Gupta *et al.*, 2013). Once dissociated from G-actin, MRTF-A translocates to the nucleus, where it acts as a master regulator of TGF- β induced EMT by upregulating genes associated with myofibroblasts, including MMP9 (Small *et al.*, 2010) (Gupta *et al.*, 2013). MLC2, a direct substrate of ROCK, was not observed to be phosphorylated in TG:JNJ rat LECs. Therefore, the Rho/ROCK pathway seemed to be inactive, and the downstream effect of MRTF-A nuclear translocation should not occur. However, we observed that the nuclear localization of MRTF-A was notably reduced, not inhibited, in TG:JNJ in comparison to TG rat LECs (Figure 23). The reduced localization of MRTF-A to the nucleus in TG:JNJ, not the lack of nuclear MRTF-A as seen in DMSO control and JNJ LECs (Figure 23), suggests that the absence of MMP9 confers resistance against TGF- β 2 induced EMT. The presence of some MRTF-A in the nucleus in TG:JNJ LECs indicates that other TGF- β 2 induced signalling pathways, that are not dependent on MMP9, could also cause the nuclear translocation of MRTF-A. With a greater concentration of TGF- β 2 or longer duration of TGF- β 2 stimulation, it may be possible to overcome the inhibitory effects of the MMP9 deficiency. This observation may explain why 25% of transgenic mice that overexpressed TGF- β 1 specifically in the lens, and thus have been exposed to elevated amounts of TGF- β since embryogenesis, and were on a

MMP9KO background (TG:MMP9KO) were able to develop ASC. The fibrotic plaques in the TG:MMP9KO mice were, however, smaller in size when compared to transgenic TGF- β 1 overexpressing mice (Korol *et al.*, 2014).

5.2 Future Directions

There are three main directions in which future investigations into the role MMP9 plays in the regulation of actin polymerization can be carried out. The first is to further investigate the proteins that were differentially regulated by the lack of MMP9. The second is to study other major TGF- β signalling pathways that could be regulated by MMP9. The third is to elucidate the roles of identified MMP9-dependent proteins during TGF- β induced EMT in LECs either through inhibitory means or with *in vivo* studies.

5.2.1 Additional investigations of the differentially regulated proteins from the cytoskeletal protein array

Further validation studies can be carried out for the other 5 proteins that were differentially regulated by the lack of MMP9. Although some of these proteins were not upregulated by 1.5-fold or greater, but the confirmation of their lack of upregulation between TGF- β treated and untreated MMP9 deficient models will add to the knowledge of the role of MMP9 during TGF- β 2-induced EMT in LECs.

5.2.2. Investigation into other potential MMP9-dependent pathways

In this study, we have demonstrated that MMP9 regulates actin polymerization and cytoskeletal remodeling during TGF- β 2-induced EMT via cortactin and the Rho/ROCK pathway. However, the canonical Smad (Miyazono, 2000), Wnt/Frizzled, and Ras/Raf/MEK/ERK pathways, which are also activated during TGF- β 2-induced EMT (Guarino *et al.*, 2009) (Lee and Nelson, 2012), should also be studied in MMP9 deficient models as they

offer alternative paths for TGF- β 2-induced EMT progression and stress fibre formation. The understanding of these pathways in MMP9 models can help clarify which pathways, and how much stimulation of such pathways, can overcome the EMT inhibitory effects offered by the lack of MMP9.

5.2.3. Investigation into mechanisms which MMP9 regulates proteins involved in actin polymerization and cell migration

This thesis has identified that the upregulation and delocalization of cortactin, the activation of FAK and the phosphorylation of MLC2 may be regulated by MMP9 during TGF- β induced EMT in the lens as these events were not observed in TGF- β 2 treated MMP9 deficient models. Furthermore, the lack of α SMA and F-actin stress fibre formation upon TGF- β 2 stimulation in MMP9 deficient models have been attributed to the absence of these proteins' roles in actin polymerization and cytoskeletal remodelling. However, the exact mechanisms by which MMP9 regulates these proteins are not well understood. Therefore, future studies can look into the inhibition of the expression or activation of the selected proteins either with KO models or with commercially available inhibitors to see if the inactivation of the selected proteins can alone prevent TGF- β 2-induced EMT. In addition, if the expression or activation of a protein is not notably different between TGF- β 2 treated MMP9 deficient LECs and untreated control LECs, then perhaps the exogenous protein can be added to the LEC culture to see if TGF- β 2-induced EMT can be restored. Lastly, *in vivo* or *ex vivo* MMP9 rescue studies can be conducted by co-treating MMP9-deficient LECs with TGF- β and an exogenous source of recombinant MMP9 to see if TGF- β 2-induced EMT can be restored.

5.3 Conclusion

The novel MMP9-specific inhibitor, JNJ0966, was confirmed to be effective at preventing TGF- β 2-induced EMT in rat LEC explants. Therefore, JNJ0966 treated rat LEC explants were used as a more efficient MMP9 deficiency model rather than LEC explants from transgenic MMP9KO mice. Results from immunofluorescence western blot validation studies using rat LECs and JNJ0966 showed similar upregulation patterns of selected proteins, cortactin, FAK, LIMK1 and MLC2, from the cytoskeletal protein array with one exception: FAK was upregulated in TG:JNJ in comparison to JNJ rat LECs. However, FAK was not activated in TG:JNJ to exert its downstream effects. Interestingly, the localizations of overall and activated LIMK1 were observed to be nuclear, which might diminish its cytoplasmic role in actin stabilization. The downstream signalling effects of the other three selected proteins, cortactin, FAK and MLC2 include actin polymerization, cell migration, contractility and cell elongation, which are all features of myofibroblasts that implicate PCO (Wormstone, 2002). Western blot and immunofluorescence analyses revealed an absence of cortactin upregulation, FAK activation and MLC phosphorylation in rat LECs that were pre-treated with JNJ0966 and then treated with TGF- β 2. Therefore, MMP9 might regulate actin polymerization and cytoskeletal remodelling during TGF- β 2-induced EMT through these proteins. Lastly, a major pathway involved in cytoskeletal remodelling during TGF- β implicated EMT is the Rho/ROCK pathway. The downstream effector of the Rho/ROCK pathway, MRTF-A, was thus assessed. MRTF-A was observed to be substantially reduced in the nuclear compartment of TG:JNJ LECs, demonstrating that the lack of MMP9 may offer resistance, not inhibition, against TGF- β 2-induced EMT and lens fibrosis.

APPENDIX

A1: Treatment of Mouse LEC Explants

Wildtype and MMP9KO mouse LEC explants were treated with 500pg/mL of recombinant human TGF- β 2 (R&D Systems, Minneapolis, MN, USA) or left untreated for 72 hours in 2mL of media. Experiment performed by Dr. Aftab Taiyab.

A2: Phalloidin Staining

Steps for fixing, permeabilizing and blocking mouse LEC explants were the same as in section 3.2, F-actin was probed for by incubating the explants with phalloidin conjugated to Alexa Fluor®568 for 2 hours at room temperature. The explants were washed three times with PBS and mounted the same way as in section 3.2. Fluorescence was detected using Leica DM6 fluorescence microscope at 40X. ($n = 3$ experiments, where $n \geq 3$ explants per treatment were used for each experiment).

A3: NanoString Analysis

Wildtype (WT) ($n = 4$ experiments, where $n = 3$ lenses per experiment), TGF- β 1 overexpressing transgenic (TGF β ^{tg}) ($n = 4$ experiments, where $n = 3$ lenses per experiment) or TGF β ^{tg} mice on the MMP9KO background (TG:MMP9KO) ($n = 4$ experiments, where $n = 3$ lenses per experiment) at 1.5-2 months of age were sacrificed and their eyes removed. RNA was isolated from the extracted lenses and expression profiling was completed using a 184-gene probe-set custom-designed array on the NanoString nCounter gene expression system, which captures and counts individual mRNA transcripts. The nSolver software was used to normalize the data to the total RNA count, and the ratios of mRNA expression were calculated using the normalized data where one set of WT was used as the reference. Microsoft Excel was used to average the normalized mRNA expression ratios and calculate the standard deviations and p-values.

A4: Cytoskeletal Protein Array

An equal number of explants ($n = 16$ explants per treatment) were obtained from 21 – 28 days old male and female mice pups of each genotype (wildtype or MMP9KO). The explants were treated with TGF- β 2 (500 pg/mL) or left untreated for 72 hours. Following treatment, protein was harvested for cytoskeletal protein array analyses (Fullmoon Biosystem, San Francisco, CA) ($n = 3$ experiments, 10 μ g of protein per treatment was used for each experiment). The protein array is focused on proteins involved in actin polymerization and provides the expression of total protein and its active counterparts in the system. The protein expression signals were normalized to the median signal of the endogenous control, GAPDH. The average protein expression levels, standard deviations and p-values were calculated from the normalized protein expression levels by using Microsoft Excel. The comparative ratios of protein expression between the TGF- β 2 treated (TG) and untreated (control) wildtype explants, and between the TGF- β 2 treated (MMP9KO-TG) and untreated MMP9KO (un-MMP9KO) explants were also calculated using Microsoft Excel. Experiment performed by Aftab Taiyab.

REFERENCES

- Andley, U. P. (2008). The lens epithelium: Focus on the expression and function of the α -crystallin chaperones. *The International Journal of Biochemistry & Cell Biology*, 40(3), 317–323. <https://doi.org/10.1016/j.biocel.2007.10.034>
- Ask, K., Bonniaud, P., Maass, K., Eickelberg, O., Margetts, P. J., Warburton, D., Groffen, J., Gauldie, J., & Kolb, M. (2008). Progressive pulmonary fibrosis is mediated by TGF- β isoform 1 but not TGF- β 3. *The International Journal of Biochemistry & Cell Biology*, 40(3), 484–495. <https://doi.org/10.1016/j.biocel.2007.08.016>
- Bamburg, J. R., & Bernstein, B. W. (2010). Roles of ADF/cofilin in actin polymerization and beyond. *F1000 Biology Reports*, 2. Published. <https://doi.org/10.3410/b2-62>
- Banh, A., Deschamps, P. A., Gauldie, J., Overbeek, P. A., Sivak, J. G., & West-Mays, J. A. (2006). Lens-Specific Expression of TGF- β Induces Anterior Subcapsular Cataract Formation in the Absence of Smad3. *Investigative Ophthalmology & Visual Science*, 47(8), 3450. <https://doi.org/10.1167/iovs.05-1208>
- Batur, M., Gül, A., Seven, E., Can, E., & Yaşar, T. (2016). Posterior Capsular Opacification in Preschool- and School-Age Patients after Pediatric Cataract Surgery without Posterior Capsulotomy. *Türk Oftalmoloji Dergisi*, 46(5), 205–208. <https://doi.org/10.4274/tjo.24650>
- Billotte, C., & Berdeaux, G. (2004). Adverse clinical consequences of neodymium:YAG laser treatment of posterior capsule opacification. *Journal of Cataract and Refractive Surgery*, 30(10), 2064–2071. <https://doi.org/10.1016/j.jcrs.2004.05.003>
- Chakraborti, S., Mandal, M., Das, S., Mandal, A., & Chakraborti, T. (2003). Regulation of matrix metalloproteinases: an overview. *Molecular and Cellular Biochemistry*, 253(1/2), 269–285. <https://doi.org/10.1023/a:1026028303196>
- Chen, Q., Gimple, R. C., Li, G., Chen, J., Wu, H., Li, R., Xie, J., & Xu, B. (2019). LIM kinase 1 acts as a profibrotic mediator in permanent atrial fibrillation patients with valvular heart disease. *Journal of Biosciences*, 44(1). <https://doi.org/10.1007/s12038-018-9825-7>
- Cheng, C., Nowak, R. B., & Fowler, V. M. (2017). The lens actin filament cytoskeleton: Diverse structures for complex functions. *Experimental Eye Research*, 156, 58–71. <https://doi.org/10.1016/j.exer.2016.03.005>
- Cicchini, C., Laudadio, I., Citarella, F., Corazzari, M., Steindler, C., Conigliaro, A., . . . Tripodi, M. (2008). TGF β -induced EMT requires focal adhesion kinase (FAK) signaling. *Experimental Cell Research*, 314(1), 143–152. <https://doi.org/10.1016/j.yexcr.2007.09.005>
- Daly, R. (2004). Cortactin signalling and dynamic actin networks. *Biochemical Journal*, 382(1), 13–25. <https://doi.org/10.1042/bj20040737>
- Dwivedi, D. J., Pino, G., Banh, A., Nathu, Z., Howchin, D., Margetts, P., . . . West-Mays, J. A. (2006). Matrix Metalloproteinase Inhibitors Suppress Transforming Growth Factor- β -Induced Subcapsular Cataract Formation. *The American Journal of Pathology*, 168(1), 69–79. <https://doi.org/10.2353/ajpath.2006.041089>
- Eldred, J. A., Dawes, L. J., & Wormstone, I. M. (2011). The lens as a model for fibrotic disease. *Philosophical Transactions of the Royal Society B: Biological Sciences*, 366(1568), 1301–1319. <https://doi.org/10.1098/rstb.2010.0341>
- Gordon-Thomson, C., de Longh, R. U., Hales, A. M., Chamberlain, C. G., & McAvoy, J. W. (1998). Differential cataractogenic potency of TGF-beta1, -beta2, and -beta3 and their expression in the postnatal rat eye. *Investigative Ophthalmology & Visual Science*, 39(8), 1399–1409.

- Gorovoy, M., Koga, T., Shen, X., Jia, Z., Yue, B. Y., & Voyno-Yasenetskaya, T. (2008). Downregulation of LIM kinase 1 suppresses ocular inflammation and fibrosis. *Molecular Vision*, *14*, 1951–1959.
- Grigera, P. R., Jeffery, E. D., Martin, K. H., Shabanowitz, J., Hunt, D. F., & Parsons, J. T. (2005). FAK phosphorylation sites mapped by mass spectrometry. *Journal of Cell Science*, *118*(21), 4931–4935. <https://doi.org/10.1242/jcs.02696>
- Guarino, M., Tosoni, A., & Nebuloni, M. (2009). Direct contribution of epithelium to organ fibrosis: epithelial-mesenchymal transition. *Human Pathology*, *40*(10), 1365–1376. <https://doi.org/10.1016/j.humpath.2009.02.020>
- Gupta, M., Korol, A., & West-Mays, J. A. (2013). Nuclear translocation of myocardin-related transcription factor-A during transforming growth factor beta-induced epithelial to mesenchymal transition of lens epithelial cells. *Molecular Vision*, *19*, 1017–1028.
- Hales, A. M. H., Chamberlain, C. G., & McAvoy, J. W. (1995). Cataract induction in lenses cultured with transforming growth factor-beta. *Investigative Ophthalmology & Visual Science*, *36*, 1709–1713.
- Hay, E. D., & Zuk, A. (1995). Transformations between epithelium and mesenchyme: Normal, pathological, and experimentally induced. *American Journal of Kidney Diseases*, *26*(4), 678–690. [https://doi.org/10.1016/0272-6386\(95\)90610-X](https://doi.org/10.1016/0272-6386(95)90610-X)
- Haynes, J., Srivastava, J., Madson, N., Wittmann, T., & Barber, D. L. (2011). Dynamic actin remodeling during epithelial–mesenchymal transition depends on increased moesin expression. *Molecular Biology of the Cell*, *22*(24), 4750–4764. <https://doi.org/10.1091/mbc.e11-02-0119>
- Hsu, J. Y. C., Bourguignon, L. Y. W., Adams, C. M., Peyrollier, K., Zhang, H., Fandel, T., Cun, C. L., Werb, Z., & Noble-Haeusslein, L. J. (2008). Matrix Metalloproteinase-9 Facilitates Glial Scar Formation in the Injured Spinal Cord. *Journal of Neuroscience*, *28*(50), 13467–13477. <https://doi.org/10.1523/jneurosci.2287-08.2008>
- Hu, H. H., Chen, D. Q., Wang, Y. N., Feng, Y. L., Cao, G., Vaziri, N. D., & Zhao, Y. Y. (2018). New insights into TGF- β /Smad signaling in tissue fibrosis. *Chemico-Biological Interactions*, *292*, 76–83. <https://doi.org/10.1016/j.cbi.2018.07.008>
- Kalluri, R., & Weinberg, R. A. (2009). The basics of epithelial-mesenchymal transition. *Journal of Clinical Investigation*, *119*(6), 1420–1428. <https://doi.org/10.1172/jci39104>
- Kass, L., Erler, J. T., Dembo, M., & Weaver, V. M. (2007). Mammary epithelial cell: Influence of extracellular matrix composition and organization during development and tumorigenesis. *The International Journal of Biochemistry & Cell Biology*, *39*(11), 1987–1994. <https://doi.org/10.1016/j.biocel.2007.06.025>
- Kobayashi, M., Tokuda, K., Kobayashi, Y., Yamashiro, C., Uchi, S. H., Hatano, M., & Kimura, K. (2019). Suppression of Epithelial-Mesenchymal Transition in Retinal Pigment Epithelial Cells by an MRTF-A Inhibitor. *Investigative Ophthalmology & Visual Science*, *60*(2), 528. <https://doi.org/10.1167/iovs.18-25678>
- Korol, A. (2017, November). *The role of cytoskeletal signaling in lens emt*. McMaster University.
- Korol, A., Pino, G., Dwivedi, D., Robertson, J. V., Deschamps, P. A., & West-Mays, J. A. (2014). Matrix Metalloproteinase-9–Null Mice Are Resistant to TGF- β –Induced Anterior Subcapsular Cataract Formation. *The American Journal of Pathology*, *184*(7), 2001–2012. <https://doi.org/10.1016/j.ajpath.2014.03.013>

- Korol, A., Taiyab, A., & West-Mays, J. A. (2016). RhoA/ROCK Signaling Regulates TGF β -Induced Epithelial-Mesenchymal Transition of Lens Epithelial Cells through MRTF-A. *Molecular Medicine*, 22(1), 713–723. <https://doi.org/10.2119/molmed.2016.00041>
- Lee, E. H., & Joo, C. K. (1999). Role of transforming growth factor-beta in transdifferentiation and fibrosis of lens epithelial cells. *Investigative Ophthalmology & Visual Science*, 40, 2025–2032.
- Lee, K., & Nelson, C. M. (2012). New Insights into the Regulation of Epithelial–Mesenchymal Transition and Tissue Fibrosis. *International Review of Cell and Molecular Biology*, 294, 171–221. <https://doi.org/10.1016/b978-0-12-394305-7.00004-5>
- Lim, S. T. S. (2013). Nuclear FAK: a new mode of gene regulation from cellular adhesions. *Molecules and Cells*, 36(1), 1–6. <https://doi.org/10.1007/s10059-013-0139-1>
- Liu, L., Ye, Y., & Zhu, X. (2019). MMP-9 secreted by tumor associated macrophages promoted gastric cancer metastasis through a PI3K/AKT/Snail pathway. *Biomedicine & Pharmacotherapy*, 117, 109096. <https://doi.org/10.1016/j.biopha.2019.109096>
- Lovicu, F., Shin, E., & McAvoy, J. (2016). Fibrosis in the lens. Sprouty regulation of TGF β -signaling prevents lens EMT leading to cataract. *Experimental Eye Research*, 142, 92–101. <https://doi.org/10.1016/j.exer.2015.02.004>
- Massova, I., Fridman, R., & Mobashery, S. (1997). Structural Insights into the Catalytic Domains of Human Matrix Metalloprotease-2 and Human Matrix Metalloprotease-9: Implications for Substrate Specificities. *Journal of Molecular Modeling*, 3(1), 17–30. <https://doi.org/10.1007/s008940050021>
- McConnell, B. V., Koto, K., & Gutierrez-Hartmann, A. (2011). Nuclear and cytoplasmic LIMK1 enhances human breast cancer progression. *Molecular Cancer*, 10(1), 75. <https://doi.org/10.1186/1476-4598-10-75>
- Mitra, S. K., Hanson, D. A., & Schlaepfer, D. D. (2005). Focal adhesion kinase: in command and control of cell motility. *Nature Reviews Molecular Cell Biology*, 6(1), 56–68. <https://doi.org/10.1038/nrm1549>
- Miyazono, K. (2000). Positive and negative regulation of TGF-beta signaling. *Journal of Cell Science*, 113(7), 1101–1109. <https://doi.org/10.1242/jcs.113.7.1101>
- Nathu, Z., Dwivedi, D. J., Reddan, J. R., Sheardown, H., Margetts, P. J., & West-Mays, J. A. (2009). Temporal changes in MMP mRNA expression in the lens epithelium during anterior subcapsular cataract formation. *Experimental Eye Research*, 88(2), 323–330. <https://doi.org/10.1016/j.exer.2008.08.014>
- O'Connor, J. W., Riley, P. N., Nalluri, S. M., Ashar, P. K., & Gomez, E. W. (2015). Matrix Rigidity Mediates TGF β 1-induced Epithelial-Myofibroblast Transition by Controlling Cytoskeletal Organization and MRTF-A Localization. *Journal of Cellular Physiology*, 230(8), 1829–1839. <https://doi.org/10.1002/jcp.24895>
- Ohashi, K., Nagata, K., Maekawa, M., Ishizaki, T., Narumiya, S., & Mizuno, K. (2000). Rho-associated Kinase ROCK Activates LIM-kinase 1 by Phosphorylation at Threonine 508 within the Activation Loop. *Journal of Biological Chemistry*, 275(5), 3577–3582. <https://doi.org/10.1074/jbc.275.5.3577>
- Olson, E. N., & Nordheim, A. (2010). Linking actin dynamics and gene transcription to drive cellular motile functions. *Nature Reviews Molecular Cell Biology*, 11(5), 353–365. <https://doi.org/10.1038/nrm2890>

- Ort, V., & Howard, D. (n.d.). *The Development of the Eye*. New York University. Retrieved October 14, 2019, from http://education.med.nyu.edu/courses/macrostructure/lectures/lec_images/eye.html#obj
- Parsons, J. T. (2003). Focal adhesion kinase: the first ten years. *Journal of Cell Science*, *116*(8), 1409–1416. <https://doi.org/10.1242/jcs.00373>
- Parsons, J. T., Martin, K. H., Slack, J. K., Taylor, J. M., & Weed, S. A. (2000). Focal Adhesion Kinase: a regulator of focal adhesion dynamics and cell movement. *Oncogene*, *19*(49), 5606–5613. <https://doi.org/10.1038/sj.onc.1203877>
- Prunier, C., Prudent, R., Kapur, R., Sadoul, K., & Lafanechère, L. (2017). LIM kinases: cofilin and beyond. *Oncotarget*, *8*(25), 41749–41763. <https://doi.org/10.18632/oncotarget.16978>
- Raj, S. M., Vasavada, A. R., Johar, S. R. K., Vasavada, V. A., & Vasavada, V. A. (2007). Post-Operative Capsular Opacification: A Review. *International Journal of Biomedical Science: IJBS*, *3*(4), 237–250.
- Saika, S., Kono-Saika, S., Ohnishi, Y., Sato, M., Muragaki, Y., Ooshima, A., Flanders, K. C., Yoo, J., Anzano, M., Liu, C. Y., Kao, W. W., & Roberts, A. B. (2004). Smad3 Signaling Is Required for Epithelial-Mesenchymal Transition of Lens Epithelium after Injury. *The American Journal of Pathology*, *164*(2), 651–663. [https://doi.org/10.1016/s0002-9440\(10\)63153-7](https://doi.org/10.1016/s0002-9440(10)63153-7)
- Scannevin, R. H., Alexander, R., Haarlander, T. M., Burke, S. L., Singer, M., Huo, C., Zhang, Y. M., Maguire, D., Spurlino, J., Deckman, I., Carroll, K. I., Lewandowski, F., Devine, E., Dzordzorme, K., Tounge, B., Milligan, C., Bayoumy, S., Williams, R., Schalk-Hihi, C., . . . Rhodes, K. J. (2017). Discovery of a highly selective chemical inhibitor of matrix metalloproteinase-9 (MMP-9) that allosterically inhibits zymogen activation. *Journal of Biological Chemistry*, *292*(43), 17963–17974. <https://doi.org/10.1074/jbc.m117.806075>
- Schwock, J., & Dhani, N. (2011, March). *PTK2 (PTK2 protein tyrosine kinase 2)*. Atlas of Genetics and Cytogenetics in Oncology and Haematology. http://atlasgeneticsoncology.org/Genes/GC_PTK2.html
- Scott, R. W., & Olson, M. F. (2007). LIM kinases: function, regulation and association with human disease. *Journal of Molecular Medicine*, *85*(6), 555–568. <https://doi.org/10.1007/s00109-007-0165-6>
- Sheikh, F., Lyon, R. C., & Chen, J. (2015). Functions of myosin light chain-2 (MYL2) in cardiac muscle and disease. *Gene*, *569*(1), 14–20. <https://doi.org/10.1016/j.gene.2015.06.027>
- Shiwen, X., Stratton, R., Nikitorowicz-Buniak, J., Ahmed-Abdi, B., Ponticos, M., Denton, C., Abraham, D., Takahashi, A., Suki, B., Layne, M. D., Lafyatis, R., & Smith, B. D. (2015). A Role of Myocardin Related Transcription Factor-A (MRTF-A) in Scleroderma Related Fibrosis. *PLOS ONE*, *10*(5), e0126015. <https://doi.org/10.1371/journal.pone.0126015>
- Šikić, H., Shi, Y., Lubura, S., & Bassnett, S. (2017). A full lifespan model of vertebrate lens growth. *Royal Society Open Science*, *4*(1), 160695. <https://doi.org/10.1098/rsos.160695>
- Small, E. M. (2012). The Actin–MRTF–SRF Gene Regulatory Axis and Myofibroblast Differentiation. *Journal of Cardiovascular Translational Research*, *5*(6), 794–804. <https://doi.org/10.1007/s12265-012-9397-0>
- Small, E. M., Thatcher, J. E., Sutherland, L. B., Kinoshita, H., Gerard, R. D., Richardson, J. A., DiMaio, J. M., Sadek, H., Kuwahara, K., & Olson, E. N. (2010). Myocardin-Related Transcription Factor-A Controls Myofibroblast Activation and Fibrosis in Response to Myocardial Infarction. *Circulation Research*, *107*(2), 294–304. <https://doi.org/10.1161/circresaha.110.223172>

- Sponer, U., Pieh, S., Soleiman, A., & Skorpik, C. (2005). Upregulation of $\alpha\text{v}\beta\text{6}$ integrin, a potent TGF- β 1 activator, and posterior capsule opacification. *Journal of Cataract and Refractive Surgery*, 31(3), 595–606. <https://doi.org/10.1016/j.jcrs.2004.05.058>
- Stamenkovic, I. (2003). Extracellular matrix remodelling: the role of matrix metalloproteinases. *The Journal of Pathology*, 200(4), 448–464. <https://doi.org/10.1002/path.1400>
- Stockis, J., Colau, D., Coulie, P. G., & Lucas, S. (2009). Membrane protein GARP is a receptor for latent TGF- β on the surface of activated human Treg. *European Journal of Immunology*, 39(12), 3315–3322. <https://doi.org/10.1002/eji.200939684>
- Taiyab, A., Holms, J., & West-Mays, J. A. (2019). β -Catenin/Smad3 Interaction Regulates Transforming Growth Factor- β -Induced Epithelial to Mesenchymal Transition in the Lens. *International Journal of Molecular Sciences*, 20(9), 2078. <https://doi.org/10.3390/ijms20092078>
- Tholozan, F. M., & Quinlan, R. A. (2007). Lens cells: More than meets the eye. *The International Journal of Biochemistry & Cell Biology*, 39(10), 1754–1759. <https://doi.org/10.1016/j.biocel.2007.06.021>
- Vision impairment and blindness*. (2021, February 26). World Health Organization. <https://www.who.int/news-room/fact-sheets/detail/blindness-and-visual-impairment>
- Vu, T. H. (2001). Don't mess with the matrix. *Nature Genetics*, 28(3), 202–203. <https://doi.org/10.1038/90023>
- Weaver, M. S., Toida, N., & Sage, E. H. (2007). Expression of integrin-linked kinase in the murine lens is consistent with its role in epithelial-mesenchymal transition of lens epithelial cells in vitro. *Molecular Vision*, 13, 707–718.
- Weed, S. A., Karginov, A. V., Schafer, D. A., Weaver, A. M., Kinley, A. W., Cooper, J. A., & Parsons, J. T. (2000). Cortactin Localization to Sites of Actin Assembly in Lamellipodia Requires Interactions with F-Actin and the Arp2/3 Complex. *Journal of Cell Biology*, 151(1), 29–40. <https://doi.org/10.1083/jcb.151.1.29>
- West-Mays, J. A. (2014). The Lens Capsule: Synthesis, Remodeling and MMPs. In A. Korol (Ed.), *Lens Epithelium and Posterior Capsular Opacification* (pp. 39–57). Springer.
- West-Mays, J. A., Pino, G., & Lovicu, F. J. (2010). Development and use of the lens epithelial explant system to study lens differentiation and cataractogenesis. *Progress in Retinal and Eye Research*, 29(2), 135–143. <https://doi.org/10.1016/j.preteyeres.2009.12.001>
- West-Mays, J. A., & Sheardown, H. (2010). Posterior Capsule Opacification. In *Ocular Disease Mechanisms and Management* (1st ed., pp. 238–242). Amsterdam, The Netherlands: Elsevier.
- Why Use Antibiotics in Cell Culture?* (n.d.). <https://www.sigmaaldrich.com/NL/En/Technical-Documents/Technical-Article/Cell-Culture-and-Cell-Culture-Analysis/Mammalian-Cell-Culture/Antibiotics-in-Cell-Culture>. Retrieved July 10, 2021, from <https://www.sigmaaldrich.com/NL/en/technical-documents/technical-article/cell-culture-and-cell-culture-analysis/mammalian-cell-culture/antibiotics-in-cell-culture>
- Wormstone, I. M. (2002). Posterior Capsule Opacification: A Cell Biological Perspective. *Experimental Eye Research*, 74(3), 337–347. <https://doi.org/10.1006/exer.2001.1153>
- Yang, N., & Mizumo, K. (1999). Nuclear export of LIM-kinase 1, mediated by two leucine-rich nuclear-export signals within the PDZ domain. *Biochemical Journal*, 338(3), 793–798. <https://doi.org/10.1042/bj3380793>

- Yu, C. W. M., Treisman, R., Bailly, M., & Khaw, P. T. (2014). The Role of the MRTF-A/SRF Pathway in Ocular Fibrosis. *Investigative Ophthalmology & Visual Science*, *55*(7), 4560. <https://doi.org/10.1167/iovs.14-14692>
- Yu, Q., & Stamenkovic, I. (2000). Cell surface-localized matrix metalloproteinase-9 proteolytically activates TGF- β and promotes tumor invasion and angiogenesis. *Genes & Development*, *14*(2), 163–176.
- Zhou, Y., Huang, X., Hecker, L., Kurundkar, D., Kurundkar, A., Liu, H., . . . Thannickal, V. J. (2013). Inhibition of mechanosensitive signaling in myofibroblasts ameliorates experimental pulmonary fibrosis. *Journal of Clinical Investigation*, *123*(3), 1096–1108. <https://doi.org/10.1172/jci66700>